Magi Brian Indrek (Orcid ID: 0000-0001-8131-0083)

Full Title: The Ensemble Oceanic Nino Index

Short Title: Ensemble ONI

Eric J. Webb[1], Brian I. Magi[1]

[1]University of North Carolina at Charlotte, Department of Geography and Earth Sciences, Charlotte, NC.

Corresponding author: Brian Magi (brian.magi@uncc.edu), Eric Webb (ewebb14@uncc.edu)

Key Words: ENSO, Ensembles, Climate, Teleconnections (AO, NAO, MJO, ENSO, SSW, ONI, ADO, MJO), Seasonal, Decadal, Centennial, Statistical Methods

Accepted Article

This article has been accepted for publication and undergone full peer review but has not been through the copyediting, typesetting, pagination and proofreading process which may lead to differences between this version and the Version of Record. Please cite this article as doi: 10.1002/joc.7535

This article is protected by copyright. All rights reserved.

Accepted Article

Abstract

We describe a new El Nino Southern Oscillation (ENSO) index that we call the Ensemble Oceanic NINO Index (Ensemble ONI). Ensemble ONI uses monthly sea surface temperature (SST) anomalies in the NINO3.4 region from 32 input SST datasets, which form the ensemble, and our new monthly ENSO index extends from the present back to the year 1850. We use the input datasets to quantify the uncertainty in the monthly index values. The uncertainty is calculated from datasets that are not completely independent from each other, but comparing our findings to other estimates of uncertainty in SST, well-documented historical ENSO events, a detailed consideration of literature-based definitions of ENSO events, and proxy-based determinations of past ENSO events, we show that our uncertainty estimates from the ensemble of input datasets is comparable both in terms of average magnitude and time-varying trend with other studies. Similar to past research, we find that ENSO events occur every 4-5 years on average, and there have been six "Super" El Ninos (1877-78, 1888-89, 1972-73, 1982-83, 1997-98, 2015-16) that statistically rise above all other El Ninos since 1850. Finally, the time span of our work shows that El Nino events were most intense at ends of both the 19th Century and the 20th Century, with a lull in the mid-1900s, corroborating previous instrumental, written, and proxy records.

1 Introduction

El Nino Southern Oscillation (ENSO) is a mode of climate variability that results from a coupled interaction between the ocean and overlying atmosphere in the tropical Pacific Ocean (McPhaden *et al.*, 2020, Bjerknes, 1966, Neelin *et al.*, 1998, Enfield, 1989), and has remote teleconnections (Wallace and Gutzler, 1981, Dai and Wigley, 2000, Bjerknes, 1969) linked to equatorial Pacific sea surface temperature (SST) anomalies. The development of ENSO indices (e.g. Trenberth and Stepaniak, 2001, Wolter and Timlin, 2011) and their refinements (e.g. van Oldenborgh *et al.*, 2021) have helped to characterize the state of the tropical Pacific and quantitatively diagnose teleconnections (Barnston *et al.*, 1997), as well as being used to evaluate climate model output (Wang *et al.*, 2021, Fredriksen *et al.*, 2020) and constrain proxy records (McGregor *et al.*, 2013).

Accepted Article

SST anomalies in the NINO3.4 region (5°S to 5°N, 120°W to 170°W) have been found to statistically capture the state of ENSO and various ENSO teleconnections (Hanley *et al.*, 2003, Trenberth, 1997, Giese and Ray, 2011), and this motivated the creation of the Oceanic Nino Index (ONI) in the 1990s by the National Oceanic and Atmospheric Administration (NOAA) Climate Prediction Center (CPC) (Barnston *et al.*, 1997, Huang *et al.*, 2017). NOAA ONI is calculated using tri-monthly averaged SST anomalies from the Extended Reconstructed Sea Surface Temperature Version 5 (ERSSTv5; Huang *et al.*, 2017) in the NINO3.4 region with a 30-year sliding base period that is updated every five years.

In this study, we present a new ENSO index that we call the Ensemble Oceanic Nino Index (Ensemble ONI) that builds on methods similar to NOAA ONI (Barnston *et al.*, 1997, Huang *et al.*, 2017), but with significant advances. First, we include an ensemble of 32 SST reconstructions and reanalysis datasets, as opposed to relying on a single SST dataset. A similar approach has been applied to other ENSO data sources including proxies (McGregor *et al.*, 2010, Braganza *et al.*, 2009), documentary records (Quinn *et al.*, 1987), and climate models (e.g. Fredriksen *et al.*, 2020, Jiang *et al.*, 2021, Yeh *et al.*, 2012, Wang *et al.*, 2021). However, fewer ensemble-based analyses of ENSO exist for instrumental datasets and reanalysis models (e.g. Zhu *et al.*, 2012). Second, while the NOAA ONI spans 1950 to present, Ensemble ONI extends from 1850 to present. Third, we provide estimates of the uncertainty in the monthly Ensemble ONI values based on the spread across the input SST datasets, which is both an advance compared to NOAA ONI and a unique contribution to the suite of ENSO indices. Quantifying uncertainty builds on evolving discussions of parametric and structural uncertainty estimation in SST at the temporal scale of ENSO events (Huang *et al.*, 2016a) and at a range of spatial scales (Huang *et al.*, 2016b, Liu *et al.*, 2015, Kennedy *et al.*, 2019, Kennedy, 2014). After presenting our methods and results, we compare Ensemble ONI with other ENSO indices, detail and justify our uncertainty estimation, and then discuss the results in terms of both magnitude and uncertainty relative to ENSO events since 1850.

Accepted Article

2 Methods

The Ensemble ONI is an index expressed as an SST anomaly averaged over the NINO3.4 region (5°S to 5°N, 120°W to 170°W) and is calculated using an ensemble of SST datasets. The time-varying spread across input datasets is the basis for our calculation of the confidence interval in the monthly Ensemble ONI.

SST anomalies in the NINO3.4 region (5°S to 5°N, 120°W to 170°W) have been found to statistically capture the state of ENSO and various ENSO teleconnections (Hanley *et al.*, 2003, Trenberth, 1997, Giese and Ray, 2011). Furthermore, **Figure 1a** shows the empirical orthogonal function (EOF) loading region of the mean SST from COBE SST2 (Hirahara *et al.*, 2014), COBE SST (Ishii *et al.*, 2005), ERSSTv4 (Huang *et al.*, 2015), ERSSTv5 (Huang *et al.*, 2017), Kaplan V2 (Kaplan *et al.*, 1998), HadISST (Rayner *et al.*, 2003), and HadISST v2.1 (Titchner and Rayner, 2014) for the 1891-2010 time span, a period during which all datasets overlap. The NINO3.4 region is in the heart of the strongest correlation with SST variability (Barnston *et al.*, 1997), whereas other Nino regions are more variable in their loading and tend to capture other "flavors" of ENSO (Ashok *et al.*, 2007, Trenberth and Stepaniak, 2001). **Figure 1b** depicts the correlation between the Southern Oscillation Index (SOI; Troup, 1965, Ropelewski and Jones, 1987) and detrended Tropical Pacific SST anomalies over the same aforementioned period. The highest correlations between the SOI and Tropical Pacific SST anomalies overlap over the NINO3.4 region, which also suggests that the NINO3.4 region is most highly correlated with other independently derived measures of ENSO, consistent with previous work (e.g. Barnston *et al.*, 1997).

Table 1 lists the 32 observational, reanalysis, and satellite datasets we used. The temporal ranges of individual datasets vary, but we combine the SST data from 1850 to present (June 2021, currently) to build the Ensemble ONI. The monthly SST value is determined as the SST averaged in NINO3.4 with a minimum of 30% spatial completeness for a "valid" monthly value to account for datasets like HadSST4 (Kennedy *et al.*, 2019) and ICOADS R3.0 (Freeman *et al.*, 2017) that are not spatially complete. Input data

Accepted Article

reported as SST anomalies (e.g. Kaplan Extended v2, Kaplan *et al.*, 1998) are first converted to SSTs using their respective climatologies and then averaged for the NINO3.4 domain.

Similar to NOAA ONI (Barnston *et al.*, 1997), we calculate the NINO3.4 SST anomaly using 30-year climatological base periods that are updated every five years. This moving window helps minimize both the overall annual and seasonal warming trends in the NINO3.4 region to produce an ENSO index that better reflects variability in ENSO state. The 30-year base periods are centered on the years of the calculation and start in 1850, noting that the present-day period from 2003-2021 uses a non-centered 30-year base period from 1990-2019 (**Table S1**).

The 30-year climatology is calculated as the monthly median of the per-dataset NINO3.4 SST (values in **Table S2**), where we require a minimum of 75% of the 30 years to be available for the dataset to contribute to that 30-year climatological base period. We use the monthly median (as opposed to the mean) to minimize the influence of outliers in the per-dataset NINO3.4 SST anomalies since (1) we do not attempt to evaluate the quality of individual months of individual input data, and (2) we aim to calculate a statistically robust measure of the central tendency of NINO3.4 SST from the ensemble to best characterize variability in ENSO state. The number of contributing datasets to each of the 30-year climatologies vary from seven to 30, generally increasing with time. We calculate the time series of NINO3.4 SST anomalies for each dataset using our 30-year base periods applied to the 5-year period centered on the 30-year base period (**Table S1**). We then calculate the median SST anomaly across all available datasets for every month, where the maximum number of datasets for a given month is 32 (**Table 1**).

The Ensemble ONI is calculated by applying a 3-month moving average to the time series of NINO3.4 SST anomalies, centered on the reported month, per the methodology of NOAA ONI (Barnston *et al.*, 1997). For uncertainty, we calculate the 3-month moving average of the 68.27% statistical percentile range. This specific percentile range allows for a rough comparison with the magnitude of the 1-sigma range derived from the calculation

Accepted Article

of standard deviation, but avoids the need for the parametric assumption of a Gaussian distribution. We argue below that using a percentile range is important in our ensemble-of-datasets approach since both the outliers and the number of datasets are time-varying. The distribution in any given month is approximately Gaussian, but each dataset (**Table 1**) produces its own SST value for the NINO3.4 region and quality-control of individual datasets is not the aim of this work.

3 Results

Figure 2 shows the time series of Ensemble ONI, shaded to show positive values in red and negative values in blue. The overall distribution from **Figure 2** is slightly positively skewed (skewness = 0.43) from a normal distribution, with the minimum to maximum range being -2.14 to 2.81 K and the median negative and positive Ensemble ONI values being equal in magnitude at -0.44 and +0.44. Consistent with past research about ENSO state and the dynamics of the Bjerknes feedback (An and Jin, 2004, Okumura and Deser, 2010), our result shows that the strongest El Ninos are stronger than the strongest La Ninas.

The Ensemble ONI reached a centennial-scale peak in the late 1800s and again in the latter part of the record, with a relatively quiet period from the early to middle 1900s (**Figure 2**), consistent with past studies (Wolter and Timlin, 2011, Garcia-Herrera *et al.*, 2008, Giese and Ray, 2011, Ray and Giese, 2012, McGregor *et al.*, 2013). A 40-year moving average of Ensemble ONI values greater than +1 (**Figure 3**) suggests that stronger El Nino conditions are more frequent and have greater amplitudes near the turn of the 20th and 21st Centuries than in the mid-20th Century, with a period of cooler positive SST anomalies from about 1900 to 1960. This multidecadal to centennial scale nonstationary behavior in stronger El Nino conditions has been noted by other studies (Enfield and Cid S., 1991, Garcia-Herrera *et al.*, 2008). Negative SST anomalies (not shown), which would correspond to months tending toward La Nina conditions, do not exhibit any multidecadal behavior since the late 1800s.

Accepted Article

Figure 4a shows Ensemble ONI bracketed by the 15.865% and 84.135% percentile values (**Table S3**), the difference of which corresponds numerically to the 68.27% confidence interval (CI) to make this comparable, at least in terms of magnitude, with the more typically-reported standard deviation. Specifically, we report the uncertainty as half the difference of the 15.865% and 84.135% percentile values, similar to the way standard deviation is often reported as 1-sigma uncertainty. Standard deviation, however, is better interpreted when the data is normally-distributed with no influential outliers, whereas using the median and percentile range implies no parametric assumptions and is far less sensitive to outliers. Another advantage of using the percentile range as the basis for uncertainty estimation is that the time-varying asymmetry relative to the central estimate is captured, and this quantitatively reveals how the input datasets (**Table 1**) themselves sometimes lean towards more positive or negative SST anomalies (**Figure S1**). Similar to Ensemble ONI, the uncertainty is reported as a moving 3-month average.

Figure 4b shows the time series of the uncertainty in Ensemble ONI, calculated as described above so that values are numerically similar to the standard deviation, and is determined by interdataset variability in SST in the NINO3.4 region (**Figure S1**). **Figure 4b** also shows the HadSST4 (Kennedy *et al.*, 2019) total uncertainty in two spatial domains: the NINO3.4 region and an "extended" NINO3.4 region (defined as 10°S to 10°N, 80°W to 170°W). To calculate the HadSST4 total uncertainty, we propagate the gridbox-specific total uncertainty to the larger spatial regions by standard propagation of errors, following guidance in Kennedy *et al.* (2019). The so-called Extended NINO3.4 region increases the maximum number of 5° latitude by 5° longitude gridboxes to 80, compared to 20 in the NINO3.4 region, noting that only a subset of gridboxes actually have data in any particular month. The 1850-2021 average number of gridboxes with data is 10 in the NINO3.4 region and 47 in the Extended NINO3.4 region. After about 1960, the data in both regions is nearly 100% complete, but from 1850-1960, both regions are more variable, ranging from 0-75% complete. We define the Extended NINO3.4 region as a way to bound our assessment of the magnitude of Ensemble ONI uncertainty, as described in Section 4.1.

Accepted Article

Our method of estimating uncertainty arises strictly from interdataset variability, which itself is a relatively simple calculation, but is similar to an estimate structural uncertainty due to variations across multiple estimations of SST anomalies. The interdataset variability is a meaningful way to gauge uncertainty (e.g. Parker, 2016, Thorne *et al.*, 2005, Kent *et al.*, 2017) since every dataset produces its own history of SST anomalies in the NINO3.4 region and the variability reflects differences in institution-specific analysis or input choices. **Figure S1** shows how the time series of monthly NINO3.4 SST values from input datasets tend to converge in the present day but also reveals the relatively large spread in the 19th Century. Our method does not specifically capture parametric uncertainty (e.g. Liu *et al.*, 2015) due to the variability arising from parameters associated with choices we make in our calculations. However, we show below that our calculation provides reasonable estimation of overall uncertainty and argue that our method is a more efficient way to calculate uncertainty than an iterative exploration of the parameter space.

Consistent with HadSST4 uncertainty, the Ensemble ONI uncertainty decreases with time (**Figure 4b**), reflecting the increasing sampling density, quality, and consistency of SST observations (Kennedy *et al.*, 2019, Freeman *et al.*, 2017), and to some degree, the number of input datasets (**Figure 4c**). The trend in the uncertainty reflects trends in the density and quality of the instrumental record (Kennedy, 2014, Kennedy *et al.*, 2011a, Kennedy *et al.*, 2011b, Kent *et al.*, 2013, Hirahara *et al.*, 2014, O'Carroll *et al.*, 2019, Karl *et al.*, 2015, Hausfather *et al.*, 2017), but also differences that are embedded in the datasets themselves. For example, some of our input datasets (Kaplan *et al.*, 1998) used older versions of ICOADS (Woodruff *et al.*, 2011, Woodruff *et al.*, 1987) and vary in the sources of observational data. These features are part of any reanalysis or observational dataset (e.g. Parker, 2016). We argue that our ensemble approach to calculating ONI strengthens the interpretation of the central estimate by including an asymmetric confidence interval (**Figure 4a**) that captures the time-varying differences across input datasets.

While the general trend in uncertainty is downward with time, three periods of uncertainty increasing with time are evident in **Figure 4b**: Prior to the 1877-78 El Nino,

Accepted Article

and during the first and second World Wars. The increasing uncertainty before 1877-78 and WWI is largely explained by a lack of data sources and observations in NINO3.4 (Freeman *et al.*, 2017, Carella *et al.*, 2018, Thompson *et al.*, 2008, Giese *et al.*, 2010). For WWI, ships were deployed for war and often destroyed. For WWII, the increasing uncertainty was due to both a similar loss of data from ship loss and to changes in how SST observations were made. Many ships switched from insulated bucket to engine room intake (ERI) SST measurements, which have a high bias relative to bucket measurements (Kennedy *et al.*, 2019). Additionally, sampling uncertainty/bias may arise from changes in the time of day most observations were collected (**Figure S2**) due to safer wartime sampling conditions during daylight as utilization of lights on-board at night to carry out more traditional bucket measurements of SST could attract enemy ships (Freeman *et al.*, 2017, Kent *et al.*, 2017). Furthermore, how this rapid paradigm shift in SST observations was addressed varied amongst dataset curators and contributes to the uncertainty in the Ensemble ONI during this time. For example, older datasets, such as Kaplan Extended SSTv2 (Kaplan *et al.*, 1998) and HadISST (Rayner *et al.*, 2003) applied no bias correction for ERI, whereas later iterations of ERSST (Huang *et al.*, 2017) bias-corrected ship observations against nighttime marine air temperatures (Kent *et al.*, 2013) somewhat analogous to Folland *et al.* (1984), and COBE SST2 (Hirahara *et al.*, 2014) applied a global mean bias correction. We therefore assert that time-varying discrepancies between SST datasets and reanalysis reflect real changes in uncertainty over the instrumental record.

4 Discussion

4.1 Assessing uncertainty

We calculate the uncertainty in Ensemble ONI from datasets that are not completely independent from each other, so we discuss both the sensitivity of the uncertainty to the datasets themselves as well as mostly or completely independent methods to justify the magnitude and sensitivity of our uncertainty estimate. We argue that the variability across the input datasets in the NINO3.4 region (**Figure S1**) is a valuable way to calculate uncertainty (Parker, 2016) by showing our uncertainty to be both conservative and in line

Accepted Article

with the magnitude of other ways that uncertainty in ENSO state can and has been estimated.

We start by assessing the sensitivity of the uncertainty to the inclusion of reanalysis and model datasets with overlapping (non-independent) input from SST datasets. The average uncertainty in **Figure 4b** is 0.29 K, but when excluding 15 reanalysis/model datasets (datasets listed with asterisks in **Table 1**), the uncertainty actually decreases to 0.27 K (**Figure 5**). This counter-intuitive result of more dispersion when reanalysis/model datasets are included is consistent with discussions of the value of intercomparisons across what would be seemingly similar reanalysis datasets (e.g. Parker, 2016, Thorne *et al.*, 2005), and suggests that reanalysis interdependencies on SST datasets do not lead to under-dispersion of uncertainty in Ensemble ONI. A plausible explanation for this seemingly contradictory result could be that techniques applied to in situ SST data from different institutions contribute to less diversity than using the same SST dataset in different reanalysis models. Specifically, reanalysis models may have SST output that has interacted with other reanalysis model fields and may be mathematically relaxed towards the in situ SST, and there are differences in data assimilation methods, model-specific parameterizations, spatiotemporal resolution, and ensemble size (e.g. Laloyaux *et al.*, 2018). Furthermore, in situ SST datasets reconstruct SSTs in the late 19th and early-mid 20th century by assuming SST variability is the same as during the modern part of the record, whereas reanalyses-based SSTs during this same period are less reliant on this assumption than they are on aspects of the models themselves (e.g. Giese and Ray, 2011).

Although we do not show the result, we found that clustering datasets with similar progeny (e.g. interdependence on a single SST dataset, such as ERA20C, ERA20CM, NOAA20CRv3, CERA-20C, ORAS5, and ERA-5 all using HadISSTv2) also resulted in less dispersion then considering the datasets independently, especially prior to the early-mid 20th century, when the least is known about instrumentally-based ENSO variability and estimates of uncertainty should be more conservative. This is generally consistent with our discussion of the effect of reanalysis/model datasets on NINO3.4 SST dispersion.

Accepted Article

For Ensemble ONI, the largest influence of the reanalysis datasets on increasing dispersion is between about 1850-1900 (**Figure 5**) when fewer datasets (**Figure 4c**) exist to constrain the uncertainty in Ensemble ONI. Uncertainty during this period averages 0.45 K when all 32 datasets are included, but 0.37 K when excluding reanalysis/model datasets. The differences are particularly large between 1850-1880 when uncertainty averages 0.52 K (all datasets) and 0.41 K (no reanalysis/model datasets). Said another way, including reanalysis/model datasets increases uncertainty by 27% prior to 1880. From 1900-1950, the average uncertainty is about the same, while for 1950-2000 the increase averages 7% and from 2000-present, reanalysis/model datasets decrease the dispersion by 11% (**Figure 5b-d**). These results suggest that including more datasets, regardless of their interdependencies, increases dispersion in the NINO3.4 region and leads to a more conservative uncertainty range for Ensemble ONI.

A way to assess the magnitude and time-evolution of our reported uncertainty is to directly compare with the comprehensive estimate of total uncertainty from HadSST4 (Kennedy *et al.*, 2019). In a month-by-month comparison, our Ensemble ONI uncertainty is less than HadSST4 NINO3.4 uncertainty in 49% of the 1842 months, and less than HadSST4 Extended NINO3.4 uncertainty in 2.5% of the months (**Figure 4b**). The median Ensemble ONI uncertainty prior to 1950 is 0.39, while the corresponding NINO3.4 and Extended NINO3.4 uncertainties for HadSST4 are 0.36 and 0.16, respectively. After 1950, the median uncertainties are smaller and are 0.15, 0.13, and 0.05 for Ensemble ONI, HadSST4 NINO3.4, and HadSST4 Extended NINO3.4, respectively. The difference in the HadSST4 calculations arises from far fewer SST observations in the NINO3.4 region than our self-defined Extended NINO3.4 region, consistent with the documented observational minimum in the central and eastern tropical Pacific evident in ICOADS (Freeman *et al.*, 2017) and HadSST4 (Kennedy *et al.*, 2019) from the lack of shipping channels that passed through NINO3.4 before the mid-1950s. In terms of magnitude, our 1-sigma Ensemble ONI uncertainty more closely follows the HadSST4 NINO3.4 region uncertainty both before and after 1950, which is the more conservative estimate of uncertainty in the comparison.

Accepted Article

The correlation of Ensemble ONI uncertainty with HadSST4 NINO3.4 uncertainty prior to 1950 is 0.42, while after 1950 is 0.62, and similar (0.42, 0.71) for the Extended NINO3.4 region. The magnitude of the correlation is less important to this discussion than the relative comparisons. Specifically, similar correlations would suggest that using the Extended NINO3.4 region HadSST4 uncertainty as a lower bound for assessing our Ensemble ONI uncertainty is reasonable, and we interpret HadSST4 uncertainty in NINO3.4 as being close to an upper bound since multiple sources of uncertainty are included in the calculation of total uncertainty reported by Kennedy *et al.* (2019). While our uncertainty estimate for Ensemble ONI is structural (deriving from interdataset variability), we argue that because HadSST4 uncertainty (Kennedy *et al.*, 2019) in NINO3.4 is comparable, then this is evidence that our uncertainty estimate is a reasonable approximation of the true uncertainty in Ensemble ONI. Furthermore, HadSST4 uncertainty is slightly (but consistently) better correlated with our estimate of Ensemble ONI uncertainty when reanalysis/model datasets are included (Pearson correlation of 0.69 and 0.63, for NINO3.4 and Extended NINO3.4 regions) rather than excluded (0.63 and 0.56, for NINO3.4 and Extended NINO3.4 regions) from our overall calculations (**Table 1**, **Figure 5**), likely due to underdispersion when excluding the 15 reanalysis/model datasets, as discussed above.

Another method to assess the accuracy of our Ensemble ONI uncertainty (**Figure 4**) is by considering strong El Nino events that were well-documented numerically and/or through historical accounts (Kiladis and Diaz, 1986, McPhaden, 1999, L'Heureux *et al.*, 2017, Huang *et al.*, 2020, Huang *et al.*, 2016a). Since the Bjerknes feedback leading to an El Nino event is well-understood (Bjerknes, 1966, McPhaden *et al.*, 2020), we argue that the state of the tropical Pacific in NINO3.4 prior to a strong El Nino event must reflect SST anomalies that themselves suggest the initiation of the Bjerknes feedback, and that this physical requirement helps constrain the corresponding uncertainty as well. Specifically, in the summer and early fall months prior to a strong El Nino event, the NINO3.4 SST anomaly is very likely to be positive. By extension, the range of Ensemble ONI values

Accepted Article

determined by any uncertainty estimate also is unlikely to be realistic if the range extends to negative values prior to the months of the peak of any strong El Nino event.

There are several strong El Nino events prior to 1950 that serve as physical constraint on the uncertainty (**Figure 6**). The 1877-78 El Nino is among the strongest in the observational record (Huang *et al.*, 2020, Sanchez *et al.*, 2020). It has been associated with prolific drought and famine that affected India and China from 1876-77 (Lin *et al.*, 2020) when an estimated 3% of the world's population died, comparable to the impact of the 1918-19 influenza pandemic (Singh *et al.*, 2018). Furthermore, coral records from the central equatorial Pacific found evidence of significant warming in the northern Line Islands 12-18 months before the peak of the 1876-78 El Nino event in late 1877 (Sanchez *et al.*, 2020), analogous to the well-documented 2015-16 El Nino (Levine and McPhaden, 2016). Finally, observed sea level pressure (SLP) at Santiago, Chile, were already three standard deviations below normal in September 1876 and remained below 1.5 standard deviations for the rest of 1876, suggesting that a significant El Nino event was already underway prior to 1877 (Kiladis and Diaz, 1986). Therefore, the summer-fall of 1877 should have positive Ensemble ONI values. The 1899-1900 El Nino was linked to drought in India and captured the interest of Sir Gilbert Walker as he formulated the framework of the Southern Oscillation (McPhaden *et al.*, 2020). The strong 1918-19 El Nino coincided with the failure of the Indian Monsoon (Giese *et al.*, 2010, Quinn *et al.*, 1978), and the 1888-89 El Nino was associated with extreme famine in Ethiopia (Wolde-Georgis, 1997) and corroborated by global written records (e.g. Quinn, 1993, Garcia-Herrera *et al.*, 2008).

In these aforementioned cases, we assert that the summers preceding these El Nino events are physically constrained to positive Ensemble ONI values, even when the full range of uncertainty is considered (**Figure 6**). Based on that assertion, our reported uncertainty range (the 68.27% percentile range) is more appropriate than, say, a larger percentile range corresponding to the 95% interval (ie. a 2-sigma range), because the larger percentile range results in summers preceding strong El Ninos potentially having negative NINO3.4 SST anomalies. **Figure 6** highlights this discrepancy, with particular attention on the 1877-78 El Nino (**Figure 6b**). The 2-sigma uncertainty range in 1877 suggests that

Accepted Article

there was potential for a developing La Nina as late as June or July, which strongly contradicts evidence (Lin *et al.*, 2020, Sanchez *et al.*, 2020, Singh *et al.*, 2018, Kiladis and Diaz, 1986) that one of the strongest El Ninos on record (Huang *et al.*, 2020) had already begun developing. **Figure 6c** shows the 1888-89 El Nino and is a case where the 1-sigma and 2-sigma uncertainty ranges both suggest at least a positive NINO3.4 SST anomaly, but close inspection shows that even in the summer 1888, the lower bound of the 2-sigma range leans towards neutral conditions, which is also unlikely given independently-derived documentary evidence (Wolde-Georgis, 1997, Quinn, 1993, Garcia-Herrera *et al.*, 2008). **Figures 6d-e** show even clearer cases that the 2-sigma range is too conservative, producing values of NINO3.4 SST anomalies that are close to zero or even negative in the summers preceding the well-documented 1899-1900 and 1918-19 (Giese *et al.*, 2010, Quinn *et al.*, 1978) El Ninos. Hence, case studies of pre-1950s El Ninos reveal substantial evidence that the larger 2-sigma uncertainty range is not consistent with the physics of the Bjerknes feedback or with independently-derived data and records.

4.2 Evaluating ENSO events since 1850

We assess Ensemble ONI against the existing NOAA ONI available from 1950-2020 (Barnston *et al.*, 1997, Huang *et al.*, 2017) and against additional ENSO indices that begin before 1950 (**Figure S3**). Differences compared to NOAA ONI are within 0.23 K, and Ensemble ONI uncertainty (**Figure 4b**) exceeds the difference in ~75% of the months. The correlation coefficients of pre-1950 Ensemble ONI with the Relative NINO3.4 index (RelNINO; van Oldenborgh *et al.*, 2021), Cold Tongue Index (CTI; Deser and Wallace, 1987), Southern Oscillation Index (SOI; Ropelewski and Jones, 1987, Allan *et al.*, 1991, Troup, 1965), and the Bivariate EnSo Timeseries index (BEST; Smith and Sardeshmukh, 2000) are 0.78, 0.78, 0.54, and 0.89, respectively (noting we multiplied SOI by -1 for comparison with SST-based indices). Post-1950, SST-based indices have better correlations ranging from 0.71 to 0.99, almost certainly due in part to higher coverage and quality of in situ observations. The highest correlation is with NOAA ONI, which is the general methodology that Ensemble ONI is based on but NOAA ONI uses only a single input dataset. SOI is less correlated with Ensemble ONI, likely since it is based on sea-

Accepted Article

level pressure station data that contains a greater proportion of high-frequency subseasonal atmospheric variability.

The bias in Ensemble ONI relative to other indices (**Figure S3**) is variable and tends to be smaller after about 1950, as expected given the confluence of all input data sets as we move towards the present day (**Figure S1**). There is a slight, but not constant, warm bias in Ensemble ONI relative to SOI and BEST, and cold bias relative to CTI. There is a slightly larger warm bias compared with RelNINO, but the bias time series varies with notable warm biases (Ensemble ONI is warmer than RelNINO) prior to 1870 and during WWII, and cold biases in the early 1900s. The non-systematic biases suggest differences that arise from the input data itself and not simply artifacts arising from methodological differences, again speaking to the explanatory power of interdataset variability being the leading source of uncertainty in Ensemble ONI.

To better characterize ENSO events, we apply a large ensemble-based approach again, but this time to 33 literature-based definitions of ENSO, minimizing subjectivity in our interpretation of the data. These definitions of ENSO state (**Table 2**) are applied to Ensemble ONI to determine time periods that correspond to ENSO events. We apply the definitions to Ensemble ONI and count the years with ENSO events by assuming that any year, defined as the boreal winter months of December-February, is an "El Nino year" or "La Nina year" when there is at least one month that meets greater than 60% of definitions. With this simple counting method, 42 El Ninos and 35 La Ninas have occurred between 1850-2021, or about one El Nino or La Nina event every 4-5 years, which near the middle of the 2-7 year return frequency in past studies (Santoso *et al.*, 2017, Ramesh and Murtugudde, 2013, Quinn *et al.*, 1978). Applying the definitions to the Ensemble ONI calculated using the full uncertainty range (**Figure 4**) results in El Nino frequency ranging from 3 to 6 years, and La Nina frequency ranging from 3 to 9 years, which is consistent with the literature-based return frequency (e.g. McPhaden *et al.*, 2020). Using the aforementioned ENSO year and literature-based definitions, we find that the transition from El Nino to La Nina occurs about twice as frequently as La Nina to El Nino, which is also consistent with previous work (Kessler, 2002, Ohba and Watanabe, 2012, Ohba and Ueda,

Accepted Article

2009, Okumura and Deser, 2010, An and Kim, 2018, An and Kim, 2017, Choi *et al.*, 2013). **Figure 7a** shows the time series of the fraction of definitions met (values in **Table S4**).

Moving beyond literature-based definitions, we augment our evaluation of ENSO events by comparing Ensemble ONI to proxy and documentary records of both El Nino and La Nina events. Comparison of the Ensemble ONI with proxy records can also help us understand uncertainties in the instrumentally-based measures of ENSO (Kennedy, 2014, Anderson *et al.*, 2013). The power in this comparison is that proxy records are completely independent from the input data we used (**Table 1**) for Ensemble ONI, and less susceptible to potential under-dispersiveness that may arise from shared biases between SST datasets and reanalysis due to their similar methodological constructions (Kennedy, 2014, Pillar *et al.*, 2018). Challenges in comparing Ensemble ONI with proxy records are that the proxy results are reported at annual time resolution (McGregor *et al.*, 2013), they may be sensitive to manifestations or flavors of ENSO that depart from NINO3.4 (Ashok *et al.*, 2007), and they are indirectly connected to SST anomalies. As we discuss below, however, the alignment of proxy-based ENSO events with both ENSO events and their uncertainty from Ensemble ONI is excellent.

We use proxy and written records from 13 literature sources, all of which document El Ninos and 11 document La Ninas, during an overlapping period between 1850 and 1977 (McGregor *et al.*, 2010, Braganza *et al.*, 2009, Cook *et al.*, 2008, Freund *et al.*, 2019, Gergis and Fowler, 2009, Li *et al.*, 2011, Tardif *et al.*, 2019, Anderson *et al.*, 2019, Hakim *et al.*, 2016, Quinn *et al.*, 1987, Sanchez *et al.*, 2020, Stahle *et al.*, 1998, Wilson *et al.*, 2010, Dätwyler *et al.*, 2020). Most of these proxy records have different units and variables, and the written records are qualitative in their classification of ENSO. To facilitate a comparison amongst them and Ensemble ONI, we use an approach modified from Wolter and Timlin (2011) and analyze the annual percentile ranks from Ensemble ONI and from each proxy records during the 1850-1977 (**Table S5**), when they all overlap. The upper, middle, and lower terciles represent El Nino, Neutral ENSO, and La Nina respectively, except for Stahle *et al.* (1998) which is an SOI-based proxy index with the

Accepted Article

signs inverted. We then analyze the percentage of proxies that meet this percentile-based definition of ENSO as a function of time.

In **Figure 7a**, the black line overlaid on the fraction of literature-based ENSO definitions shows the fraction of the proxies (values in **Table S5**) that reported an El Nino (out of 13 proxies) or La Nina (out of 11) between 1850 and 1977, noting that the proxy results are at annual time resolution. There are 42 El Ninos and 41 La Ninas of varying strength and duration. Remarkably, there are only two ENSO events, both of which are La Ninas, that were not identified by any proxy but that met at least 50% of the literature-based definitions of being La Ninas: 1856-57 and 1903-04. The 1856-57 event has 105% uncertainty while the 1903-04 has 58% uncertainty (**Figure 4**) around the central Ensemble ONI value, where the percentages are calculated as the average uncertainty from July to March divided by the average Ensemble ONI from July to March. These are high relative to uncertainty in ENSO events in their respective time periods (93% on average from 1850-1869, and 37% from 1890-1909) so there is the possibility that the Ensemble ONI reported an overly-strong La Nina state, or that a La Nina did occur and did not manifest in the proxy records. The main conclusion from **Figure 7**, however, is that the vast majority of ENSO events are substantiated by completely independent records from multiple proxies.

Acknowledging the results of our uncertainty assessment, and of the comparisons with literature-based definitions and proxy-based findings, we take the Ensemble ONI values and categorize El Nino and La Nina events since 1850 based on the maximum Ensemble ONI during the months of October-March. We specify "Strong" El Ninos when peak values range from $+1.5℃$ to $+2.0℃$, and "Strong" La Ninas are values are less than $-1.5℃$, while "Super" El Ninos are events with peaks exceeding $+2.0℃$. Due to their climatic and large-scale impacts, Super El Ninos are a category that is discussed in the literature beyond our operational classification (Hameed *et al.*, 2018, Latif *et al.*, 2015, Chen *et al.*, 2016, Bing and Xie, 2017).

We identify six Super El Ninos (**Figure 8a**) in 1877-78, 1997-98, 2015-16, 1982-83, 1972-73, and 1888-89. The top four all sustained average Ensemble ONI values greater

Accepted Article

than +2.0°C from October-March, separating them from the 1972-73 and 1888-89 events. The top three Super El Ninos have uncertainty ranges that statistically distinguish them from other ENSO events since 1850. Furthermore, the Super El Ninos have well-documented global temperature anomalies (Morice *et al.*, 2021) and impacts (Zhu *et al.*, 2018, van der Werf *et al.*, 2004, Slingo and Annamalai, 2000). **Figure S4** shows the results in **Figure 8** but compares the magnitude of the peak ENSO event amplitude from NOAA ONI (Barnston *et al.*, 1997) and Relative NINO3.4 (van Oldenborgh *et al.*, 2021), both of which rely on a single input dataset as opposed to the 32 input datasets for Ensemble ONI. NOAA ONI top 20 results are very similar, but Relative NINO produces more super El Ninos.

Even though the 1988-89 and 1916-17 La Ninas are the strongest since 1850 (**Figure 8b**), we do not separate Super from Strong La Ninas because uncertainty in Ensemble ONI prevents a clear distinction between these and slightly weaker, but still intense, La Ninas. **Figure 8** also shows how the asymmetric uncertainty derived from interdataset variability could result in some of the top 20 ENSO events prior to 1950 shifting towards Super El Ninos (1896-97, 1902-03) or towards Moderate El Ninos (1930-31, 1899-00) as more data is considered.

All the top 20 El Nino events were recorded in the proxy records summarized in **Figure 7**, with an average of 81% of the proxies reporting an El Nino event in the top 20 years compared to an average of 52% in non-top 20 years. Similarly, all but the 1856-57 La Nina event (0 proxies noted this) were recorded in the proxy records (**Figure 7**), with an average of 77% reporting La Ninas in the matching years of top 20 La Ninas compared to an average of 46% in non-top 20 years. The interpretation is that top 20 events are more likely to be evident in documentary sources, proxy records, and physical state variables such as SST anomalies in the NINO3.4 region, and that Ensemble ONI provides realistic estimates of ENSO even when in-situ SST observations are scarce in the 19th and early-mid 20th centuries.

5 Conclusions

Accepted Article

The Ensemble Oceanic NINO Index (Ensemble ONI) uses an ensemble of input datasets to develop a new ENSO index based on NINO3.4 region SST anomalies. We use methods that are similar to the existing NOAA ONI (Barnston *et al.*, 1997), but our work incorporates an ensemble of 32 input SST datasets (**Table 1**), extends back to the year 1850 is available in near real-time, and uses the ensemble to quantify uncertainty (**Figure 2**).

Our methodology uses both a median of shifting base-period climatologies (to account for warming evident in the NINO3.4 region, **Figure S1**) and a median SST anomaly across the ensemble of 32 datasets. The choice of a median helps resist the influence of outliers that may arise in any month since 1850 within individual datasets. In other words, our methods do not attempt to diagnose issues, artifacts, or methodologies of each dataset, but instead consider what the ensemble as a whole suggests about NINO3.4 SSTs. Our methods can thus easily ingest additional data both backwards in time and as the future unfolds. A larger ensemble of values in any given month strengthens the central estimate of the Ensemble ONI, and we find that the variability across all datasets, regardless of similarities in the underlying in situ SST, produces the most conservative uncertainty range (**Figures 4-5**).

We discuss the time evolution of our estimates of uncertainty, and compare the magnitude to HadSST4 total uncertainty (Kennedy *et al.*, 2019) for the NINO3.4 region. We also advance the discussion of uncertainty estimate by arguing that our best estimates are semi-quantitatively constrained by well-documented ENSO events (**Figure 6**), a suite of 33 different literature-based definitions, and comparisons with 13 proxy records of ENSO events since 1850 (**Figure 7**). We argue that our uncertainty, which is determined from the variability across our 32-dataset ensemble, offers a way to refine future estimates of uncertainty in ENSO indices against diverse sources.

Our results show that there is a statistical distinction between Super El Ninos and Strong ones, but that the same does not apply to La Ninas. In terms of ranking, the 1877-78 El Nino is the strongest, but uncertainty in the peak magnitude of the event does not rule out the possibility that the 1982-83, 1997-98, or 2015-16 El Ninos were at least as strong,

Accepted Article

consistent with Huang *et al.* (2020). However, our findings also do not rule out the possibility that 1877-78 was even stronger than our central estimate (e.g. Sanchez *et al.*, 2020), as severe undersampling in the core of the central Pacific and similarity in methods amongst SST dataset curators may be underestimating the "true" amplitude of the event (Kaplan *et al.*, 1998). Coral records, for example, from the Fanning and Palmyra Islands (Sanchez *et al.*, 2020) suggest that the magnitude of the 1877-78 El Nino was more than one standard deviation greater than the next strongest El Nino (1997-98). In any case, those four El Ninos are very likely Super El Ninos in terms of peak magnitude, conditions averaged over boreal winter months, and documented global impacts.

Consistent with ENSO asymmetry (An and Kim, 2018), we do not make a distinction for "Super" La Ninas, but the two strongest are 1916-17 and 1988-89, with the latter being so intense that it led to the establishment of the term La Nina in literature over 30 years ago (McPhaden *et al.*, 2015, Philander, 1990). Finally, the time span of our work shows that El Nino events were more intense at the turn of both the 20th and 21st centuries, with a lull in the mid-1900s (**Figure 3**), similar to other studies (Giese and Ray, 2011, McGregor *et al.*, 2013, Wolter and Timlin, 2011), some of which have suggested this centennial-scale variability in ENSO amplitude has existed for at least the last few-several hundred years or more (Liu *et al.*, 2017, Garcia-Herrera *et al.*, 2008, Tindall *et al.*, 2016, Langton *et al.*, 2008, Li *et al.*, 2011, Enfield and Cid S., 1991), although our work does not attempt to diagnose the causal mechanism (e.g. Karnauskas *et al.*, 2012, Lewis and LeGrande, 2015) and may be underestimating centennial-scale variability (e.g. Wittenberg, 2009, Ault *et al.*, 2013).

The Ensemble ONI and its associated uncertainty (**Figure 4**) establish a reliable baseline with which to compare and possibly constrain other SST datasets, reanalysis models, proxy and documentary reconstructions, as well as climate models. Future developments of the Ensemble ONI include incorporating pre-1850s data as new records are compiled (Slivinski *et al.*, 2019, Giese *et al.*, 2016, Freeman *et al.*, 2017), exploring flavors of El Nino (Ashok *et al.*, 2007), re-calculation of ONI relative to tropical ocean warming trends (van Oldenborgh *et al.*, 2021), and further refining the uncertainty

Accepted Article

estimation for pre-1950s data. Additional or updated reanalysis or observational datasets can also be incorporated readily, and our methods be adaptable to explore other Nino regions to address dynamical interconnections (Ummenhofer *et al.*, 2011, Xie *et al.*, 2009). Finally, our methods could be adapted to combine SST data with additional dimensions (Wolter and Timlin, 2011), such as long-term records of sea level pressure (Quinn *et al.*, 1978, Cram *et al.*, 2015, Allan *et al.*, 2002, Ropelewski and Jones, 1987), for a multivariate-ensemble ENSO index.

Acknowledgements

The authors declare no conflicts of interest, and no specific sources of funding. We thank KNMI Climate Explorer for maintaining their data repository for exploring large datasets. The data used in this study are available in **Table S3**.

Accepted Article

References

Allan, R. J., Nicholls, N., Jones, P. D. & Butterworth, I. J. 1991. A Further Extension of the Tahiti-Darwin SOI, Early ENSO Events and Darwin Pressure. *Journal of Climate,* 4**,** 743-749.

Allan, R. J., Reason, C. J. C., Carroll, P. & Jones, P. D. 2002. A reconstruction of Madras (Chennai) mean sea-level pressure using instrumental records from the late 18th and early 19th centuries. *International Journal of Climatology,* 22**,** 1119-1142.

An, S.-I. & Jin, F.-F. 2004. Nonlinearity and Asymmetry of ENSO. *Journal of Climate,* 17**,** 2399-2412.

An, S.-I. & Kim, J.-W. 2017. Role of nonlinear ocean dynamic response to wind on the asymmetrical transition of El Niño and La Niña. *Geophysical Research Letters,* 44**,** 393-400.

An, S.-I. & Kim, J.-W. 2018. ENSO Transition Asymmetry: Internal and External Causes and Intermodel Diversity. *Geophysical Research Letters,* 45**,** 5095-5104.

Anderson, D., Tardif, R., Horlick, K., Erb, M., Hakim, G., Noone, D., Perkins, W. & Steig, E. 2019. Additions to the last millennium reanalysis multi-proxy database. *Data Science Journal,* 18.

Anderson, D. M., Mauk, E. M., Wahl, E. R., Morrill, C., Wagner, A. J., Easterling, D. & Rutishauser, T. 2013. Global warming in an independent record of the past 130 years. *Geophysical Research Letters,* 40**,** 189-193.

Ashok, K., Behera, S. K., Rao, S. A., Weng, H. & Yamagata, T. 2007. El Niño Modoki and its possible teleconnection. *Journal of Geophysical Research: Oceans,* 112.

Ault, T. R., Deser, C., Newman, M. & Emile-Geay, J. 2013. Characterizing decadal to centennial variability in the equatorial Pacific during the last millennium. *Geophysical Research Letters,* 40**,** 3450-3456.

Barnston, A. G., Chelliah, M. & Goldenberg, S. B. 1997. Documentation of a highly ENSO-related sst region in the equatorial pacific: Research note. *Atmosphere-Ocean,* 35**,** 367-383.

Bing, Z. & Xie, S. 2017. The 2015/16 "Super" El Niño Event and Its Climatic Impact. *Chinese Journal of Urban and Environmental Studies,* 05**,** 1750017.

Bjerknes, J. 1966. A possible response of the atmospheric Hadley circulation to equatorial anomalies of ocean temperature. *Tellus,* 18**,** 820-829.

Bjerknes, J. 1969. Atmospheric Teleconnections from the Equatorial Pacific. *Monthly Weather Review,* 97**,** 163-172.

Bove, M. C., Elsner, J. B., Landsea, C. W., Niu, X. & O'Brien, J. J. 1998. Effect of El Niño on US landfalling hurricanes, revisited. *Bulletin of the American Meteorological Society,* 79**,** 2477-2482.

Braganza, K., Gergis, J. L., Power, S. B., Risbey, J. S. & Fowler, A. M. 2009. A multiproxy index of the El Niño–Southern Oscillation, A.D. 1525–1982. *Journal of Geophysical Research: Atmospheres,* 114.

Carella, G., Kennedy, J. J., Berry, D. I., Hirahara, S., Merchant, C. J., Morak-Bozzo, S. & Kent, E. C. 2018. Estimating Sea Surface Temperature Measurement Methods

Accepted Article

Using Characteristic Differences in the Diurnal Cycle. *Geophysical Research Letters,* 45**,** 363-371.

Chen, D., Cane, M. A., Kaplan, A., Zebiak, S. E. & Huang, D. 2004. Predictability of El Niño over the past 148 years. *Nature,* 428**,** 733-736.

Chen, L., Li, T., Behera, S. K. & Doi, T. 2016. Distinctive precursory air–sea signals between regular and super El Niños. *Advances in Atmospheric Sciences,* 33**,** 996-1004.

Choi, K.-Y., Vecchi, G. A. & Wittenberg, A. T. 2013. ENSO Transition, Duration, and Amplitude Asymmetries: Role of the Nonlinear Wind Stress Coupling in a Conceptual Model. *Journal of Climate,* 26**,** 9462-9476.

Coelho, C. A. S., Uvo, C. B. & Ambrizzi, T. 2002. Exploring the impacts of the tropical Pacific SST on the precipitation patterns over South America during ENSO periods. *Theoretical and Applied Climatology,* 71**,** 185-197.

Compo, G. P., Whitaker, J. S., Sardeshmukh, P. D., Matsui, N., Allan, R. J., Yin, X., Gleason, B. E., Vose, R. S., Rutledge, G., Bessemoulin, P., Brönnimann, S., Brunet, M., Crouthamel, R. I., Grant, A. N., Groisman, P. Y., Jones, P. D., Kruk, M. C., Kruger, A. C., Marshall, G. J., Maugeri, M., Mok, H. Y., Nordli, Ø., Ross, T. F., Trigo, R. M., Wang, X. L., Woodruff, S. D. & Worley, S. J. 2011. The Twentieth Century Reanalysis Project. *Quarterly Journal of the Royal Meteorological Society,* 137**,** 1-28.

Cook, E., D'Arrigo, R. & Anchukaitis, K. ENSO reconstructions from long tree-ring chronologies: Unifying the differences. Talk presented at a special workshop on Reconciling ENSO Chronologies for the Past, 2008. https://www.ncdc.noaa.gov/paleo-search/study/8704, 15.

Cram, T. A., Compo, G. P., Yin, X., Allan, R. J., McColl, C., Vose, R. S., Whitaker, J. S., Matsui, N., Ashcroft, L., Auchmann, R., Bessemoulin, P., Brandsma, T., Brohan, P., Brunet, M., Comeaux, J., Crouthamel, R., Gleason Jr, B. E., Groisman, P. Y., Hersbach, H., Jones, P. D., Jónsson, T., Jourdain, S., Kelly, G., Knapp, K. R., Kruger, A., Kubota, H., Lentini, G., Lorrey, A., Lott, N., Lubker, S. J., Luterbacher, J., Marshall, G. J., Maugeri, M., Mock, C. J., Mok, H. Y., Nordli, Ø., Rodwell, M. J., Ross, T. F., Schuster, D., Srnec, L., Valente, M. A., Vizi, Z., Wang, X. L., Westcott, N., Woollen, J. S. & Worley, S. J. 2015. The International Surface Pressure Databank version 2. *Geoscience Data Journal,* 2**,** 31-46.

Dai, A. & Wigley, T. M. L. 2000. Global patterns of ENSO-induced precipitation. *Geophysical Research Letters,* 27**,** 1283-1286.

Dätwyler, C., Grosjean, M., Steiger, N. J. & Neukom, R. 2020. Teleconnections and relationship between the El Niño–Southern Oscillation (ENSO) and the Southern Annular Mode (SAM) in reconstructions and models over the past millennium. *Clim. Past,* 16**,** 743-756.

Dee, D. P., Uppala, S. M., Simmons, A. J., Berrisford, P., Poli, P., Kobayashi, S., Andrae, U., Balmaseda, M. A., Balsamo, G., Bauer, P., Bechtold, P., Beljaars, A. C. M., van de Berg, L., Bidlot, J., Bormann, N., Delsol, C., Dragani, R., Fuentes, M., Geer, A. J., Haimberger, L., Healy, S. B., Hersbach, H., Hólm, E. V., Isaksen, L., Kållberg, P., Köhler, M., Matricardi, M., McNally, A. P., Monge-Sanz, B. M., Morcrette, J.-J., Park, B.-K., Peubey, C., de Rosnay, P., Tavolato, C., Thépaut, J.-N. & Vitart, F.

Accepted Article

2011. The ERA-Interim reanalysis: configuration and performance of the data assimilation system. *Quarterly Journal of the Royal Meteorological Society,* 137**,** 553-597.

Deser, C. & Wallace, J. M. 1987. El Niño events and their relation to the Southern Oscillation: 1925–1986. *Journal of Geophysical Research: Oceans,* 92**,** 14189-14196.

Enfield, D. B. 1989. El Niño, past and present. *Reviews of Geophysics,* 27**,** 159-187.

Enfield, D. B. & Cid S., L. 1991. Low-Frequency Changes in El Niño-Southern Oscillation. *Journal of Climate,* 4**,** 1137-1146.

Folland, C. K., Parker, D. E. & Kates, F. E. 1984. Worldwide marine temperature fluctuations 1856–1981. *Nature,* 310**,** 670-673.

Fredriksen, H.-B., Berner, J., Subramanian, A. C. & Capotondi, A. 2020. How Does El Niño–Southern Oscillation Change Under Global Warming—A First Look at CMIP6. *Geophysical Research Letters,* 47**,** e2020GL090640.

Freeman, E., Woodruff, S. D., Worley, S. J., Lubker, S. J., Kent, E. C., Angel, W. E., Berry, D. I., Brohan, P., Eastman, R., Gates, L., Gloeden, W., Ji, Z., Lawrimore, J., Rayner, N. A., Rosenhagen, G. & Smith, S. R. 2017. ICOADS Release 3.0: a major update to the historical marine climate record. *International Journal of Climatology,* 37**,** 2211-2232.

Freund, M. B., Henley, B. J., Karoly, D. J., McGregor, H. V., Abram, N. J. & Dommenget, D. 2019. Higher frequency of Central Pacific El Niño events in recent decades relative to past centuries. *Nature Geoscience,* 12**,** 450-455.

Garcia-Herrera, R., Barriopedro, D., Hernández, E., Diaz, H. F., Garcia, R. R., Prieto, M. R. & Moyano, R. 2008. A Chronology of El Niño Events from Primary Documentary Sources in Northern Peru. *Journal of Climate,* 21**,** 1948-1962.

Gelaro, R., McCarty, W., Suárez, M. J., Todling, R., Molod, A., Takacs, L., Randles, C. A., Darmenov, A., Bosilovich, M. G., Reichle, R., Wargan, K., Coy, L., Cullather, R., Draper, C., Akella, S., Buchard, V., Conaty, A., da Silva, A. M., Gu, W., Kim, G.-K., Koster, R., Lucchesi, R., Merkova, D., Nielsen, J. E., Partyka, G., Pawson, S., Putman, W., Rienecker, M., Schubert, S. D., Sienkiewicz, M. & Zhao, B. 2017. The Modern-Era Retrospective Analysis for Research and Applications, Version 2 (MERRA-2). *Journal of Climate,* 30**,** 5419-5454.

Gergis, J. L. & Fowler, A. M. 2005. Classification of synchronous oceanic and atmospheric El Niño-Southern Oscillation (ENSO) events for palaeoclimate reconstruction. *International Journal of Climatology,* 25**,** 1541-1565.

Gergis, J. L. & Fowler, A. M. 2009. A history of ENSO events since A.D. 1525: implications for future climate change. *Climatic Change,* 92**,** 343-387.

Giese, B. S., Compo, G. P., Slowey, N. C., Sardeshmukh, P. D., Carton, J. A., Ray, S. & Whitaker, J. S. 2010. The 1918/19 El Niño. *Bulletin of the American Meteorological Society,* 91**,** 177-183.

Giese, B. S. & Ray, S. 2011. El Niño variability in simple ocean data assimilation (SODA), 1871–2008. *Journal of Geophysical Research: Oceans,* 116.

Giese, B. S., Seidel, H. F., Compo, G. P. & Sardeshmukh, P. D. 2016. An ensemble of ocean reanalyses for 1815–2013 with sparse observational input. *Journal of Geophysical Research: Oceans,* 121**,** 6891-6910.

Accepted Article

Hakim, G. J., Emile-Geay, J., Steig, E. J., Noone, D., Anderson, D. M., Tardif, R., Steiger, N. & Perkins, W. A. 2016. The last millennium climate reanalysis project: Framework and first results. *Journal of Geophysical Research: Atmospheres,* 121**,** 6745-6764.

Hameed, S. N., Jin, D. & Thilakan, V. 2018. A model for super El Niños. *Nature Communications,* 9**,** 2528.

Hanley, D. E., Bourassa, M. A., O'Brien, J. J., Smith, S. R. & Spade, E. R. 2003. A Quantitative Evaluation of ENSO Indices. *Journal of Climate,* 16**,** 1249-1258.

Hausfather, Z., Cowtan, K., Clarke, D. C., Jacobs, P., Richardson, M. & Rohde, R. 2017. Assessing recent warming using instrumentally homogeneous sea surface temperature records. *Science Advances,* 3**,** e1601207.

Hendon, H. H., Lim, E., Wang, G., Alves, O. & Hudson, D. 2009. Prospects for predicting two flavors of El Niño. *Geophysical Research Letters,* 36.

Hersbach, H., Bell, B., Berrisford, P., Hirahara, S., Horányi, A., Muñoz-Sabater, J., Nicolas, J., Peubey, C., Radu, R., Schepers, D., Simmons, A., Soci, C., Abdalla, S., Abellan, X., Balsamo, G., Bechtold, P., Biavati, G., Bidlot, J., Bonavita, M., De Chiara, G., Dahlgren, P., Dee, D., Diamantakis, M., Dragani, R., Flemming, J., Forbes, R., Fuentes, M., Geer, A., Haimberger, L., Healy, S., Hogan, R. J., Hólm, E., Janisková, M., Keeley, S., Laloyaux, P., Lopez, P., Lupu, C., Radnoti, G., de Rosnay, P., Rozum, I., Vamborg, F., Villaume, S. & Thépaut, J.-N. 2020. The ERA5 global reanalysis. *Quarterly Journal of the Royal Meteorological Society,* 146**,** 1999-2049.

Hersbach, H., Peubey, C., Simmons, A., Berrisford, P., Poli, P. & Dee, D. 2015. ERA-20CM: a twentieth-century atmospheric model ensemble. *Quarterly Journal of the Royal Meteorological Society,* 141**,** 2350-2375.

Hirahara, S., Ishii, M. & Fukuda, Y. 2014. Centennial-Scale Sea Surface Temperature Analysis and Its Uncertainty. *Journal of Climate,* 27**,** 57-75.

Huang, B., Banzon, V. F., Freeman, E., Lawrimore, J., Liu, W., Peterson, T. C., Smith, T. M., Thorne, P. W., Woodruff, S. D. & Zhang, H.-M. 2015. Extended Reconstructed Sea Surface Temperature Version 4 (ERSST.v4). Part I: Upgrades and Intercomparisons. *Journal of Climate,* 28**,** 911-930.

Huang, B., L'Heureux, M., Hu, Z.-Z. & Zhang, H.-M. 2016a. Ranking the strongest ENSO events while incorporating SST uncertainty. *Geophysical Research Letters,* 43**,** 9165-9172.

Huang, B., L'Heureux, M., Hu, Z.-Z., Yin, X. & Zhang, H.-M. 2020. How Significant Was the 1877/78 El Niño? *Journal of Climate,* 33**,** 4853-4869.

Huang, B., Thorne, P. W., Banzon, V. F., Boyer, T., Chepurin, G., Lawrimore, J. H., Menne, M. J., Smith, T. M., Vose, R. S. & Zhang, H.-M. 2017. Extended Reconstructed Sea Surface Temperature, Version 5 (ERSSTv5): Upgrades, Validations, and Intercomparisons. *Journal of Climate,* 30**,** 8179-8205.

Huang, B., Thorne, P. W., Smith, T. M., Liu, W., Lawrimore, J., Banzon, V. F., Zhang, H.-M., Peterson, T. C. & Menne, M. 2016b. Further Exploring and Quantifying Uncertainties for Extended Reconstructed Sea Surface Temperature (ERSST) Version 4 (v4). *Journal of Climate,* 29**,** 3119-3142.

Accepted Article

Ishii, M., Shouji, A., Sugimoto, S. & Matsumoto, T. 2005. Objective analyses of sea-surface temperature and marine meteorological variables for the 20th century using ICOADS and the Kobe Collection. *International Journal of Climatology,* 25**,** 865-879.

Jiang, W., Huang, P., Huang, G. & Ying, J. 2021. Origins of the Excessive Westward Extension of ENSO SST Simulated in CMIP5 and CMIP6 Models. *Journal of Climate,* 34**,** 2839-2851.

Kalnay, E., Kanamitsu, M., Kistler, R., Collins, W., Deaven, D., Gandin, L., Iredell, M., Saha, S., White, G., Woollen, J., Zhu, Y., Chelliah, M., Ebisuzaki, W., Higgins, W., Janowiak, J., Mo, K. C., Ropelewski, C., Wang, J., Leetmaa, A., Reynolds, R., Jenne, R. & Joseph, D. 1996. The NCEP/NCAR 40-Year Reanalysis Project. *Bulletin of the American Meteorological Society,* 77**,** 437-472.

Kanamitsu, M., Ebisuzaki, W., Woollen, J., Yang, S.-K., Hnilo, J. J., Fiorino, M. & Potter, G. L. 2002. NCEP–DOE AMIP-II Reanalysis (R-2). *Bulletin of the American Meteorological Society,* 83**,** 1631-1644.

Kao, H.-Y. & Yu, J.-Y. 2009. Contrasting eastern-Pacific and central-Pacific types of ENSO. *Journal of Climate,* 22**,** 615-632.

Kaplan, A., Cane, M. A., Kushnir, Y., Clement, A. C., Blumenthal, M. B. & Rajagopalan, B. 1998. Analyses of global sea surface temperature 1856–1991. *Journal of Geophysical Research: Oceans,* 103**,** 18567-18589.

Karl, T. R., Arguez, A., Huang, B., Lawrimore, J. H., McMahon, J. R., Menne, M. J., Peterson, T. C., Vose, R. S. & Zhang, H.-M. 2015. Possible artifacts of data biases in the recent global surface warming hiatus. *Science,* 348**,** 1469-1472.

Karnauskas, K. B., Smerdon, J. E., Seager, R. & González-Rouco, J. F. 2012. A Pacific Centennial Oscillation Predicted by Coupled GCMs. *Journal of Climate,* 25**,** 5943-5961.

Kennedy, J. J. 2014. A review of uncertainty in in situ measurements and data sets of sea surface temperature. *Reviews of Geophysics,* 52**,** 1-32.

Kennedy, J. J., Rayner, N. A., Atkinson, C. P. & Killick, R. E. 2019. An Ensemble Data Set of Sea Surface Temperature Change From 1850: The Met Office Hadley Centre HadSST.4.0.0.0 Data Set. *Journal of Geophysical Research: Atmospheres,* 124**,** 7719-7763.

Kennedy, J. J., Rayner, N. A., Smith, R. O., Parker, D. E. & Saunby, M. 2011a. Reassessing biases and other uncertainties in sea surface temperature observations measured in situ since 1850: 1. Measurement and sampling uncertainties. *Journal of Geophysical Research: Atmospheres,* 116.

Kennedy, J. J., Rayner, N. A., Smith, R. O., Parker, D. E. & Saunby, M. 2011b. Reassessing biases and other uncertainties in sea surface temperature observations measured in situ since 1850: 2. Biases and homogenization. *Journal of Geophysical Research: Atmospheres,* 116.

Kent, E. C., Kennedy, J. J., Smith, T. M., Hirahara, S., Huang, B., Kaplan, A., Parker, D. E., Atkinson, C. P., Berry, D. I., Carella, G., Fukuda, Y., Ishii, M., Jones, P. D., Lindgren, F., Merchant, C. J., Morak-Bozzo, S., Rayner, N. A., Venema, V., Yasui, S. & Zhang, H.-M. 2017. A Call for New Approaches to Quantifying Biases in

Accepted Article

Observations of Sea Surface Temperature. *Bulletin of the American Meteorological Society,* 98**,** 1601-1616.

Kent, E. C., Rayner, N. A., Berry, D. I., Saunby, M., Moat, B. I., Kennedy, J. J. & Parker, D. E. 2013. Global analysis of night marine air temperature and its uncertainty since 1880: The HadNMAT2 data set. *Journal of Geophysical Research: Atmospheres,* 118**,** 1281-1298.

Kessler, W. S. 2002. Is ENSO a cycle or a series of events? *Geophysical Research Letters,* 29**,** 40-1-40-4.

Kiladis, G. N. & Diaz, H. F. 1986. An Analysis of the 1877–78 ENSO Episode and Comparison with 1982–83. *Monthly Weather Review,* 114**,** 1035-1047.

L'Heureux, M. L., Takahashi, K., Watkins, A. B., Barnston, A. G., Becker, E. J., Di Liberto, T. E., Gamble, F., Gottschalck, J., Halpert, M. S., Huang, B., Mosquera-Vásquez, K. & Wittenberg, A. T. 2017. Observing and Predicting the 2015/16 El Niño. *Bulletin of the American Meteorological Society,* 98**,** 1363-1382.

Laloyaux, P., de Boisseson, E., Balmaseda, M., Bidlot, J.-R., Broennimann, S., Buizza, R., Dalhgren, P., Dee, D., Haimberger, L., Hersbach, H., Kosaka, Y., Martin, M., Poli, P., Rayner, N., Rustemeier, E. & Schepers, D. 2018. CERA-20C: A Coupled Reanalysis of the Twentieth Century. *Journal of Advances in Modeling Earth Systems,* 10**,** 1172-1195.

Langton, S. J., Linsley, B. K., Robinson, R. S., Rosenthal, Y., Oppo, D. W., Eglinton, T. I., Howe, S. S., Djajadihardja, Y. S. & Syamsudin, F. 2008. 3500 yr record of centennial-scale climate variability from the Western Pacific Warm Pool. *Geology,* 36**,** 795-798.

Latif, M., Semenov, V. A. & Park, W. 2015. Super El Niños in response to global warming in a climate model. *Climatic Change,* 132**,** 489-500.

Levine, A. F. Z. & McPhaden, M. J. 2016. How the July 2014 easterly wind burst gave the 2015–2016 El Niño a head start. *Geophysical Research Letters,* 43**,** 6503-6510.

Lewis, S. C. & LeGrande, A. N. 2015. Stability of ENSO and its tropical Pacific teleconnections over the Last Millennium. *Clim. Past,* 11**,** 1347-1360.

Li, J., Xie, S.-P., Cook, E. R., Huang, G., D'Arrigo, R., Liu, F., Ma, J. & Zheng, X.-T. 2011. Interdecadal modulation of El Niño amplitude during the past millennium. *Nature Climate Change,* 1**,** 114-118.

Lin, K. H. E., Wang, P. K., Pai, P. L., Lin, Y. S. & Wang, C. W. 2020. Historical droughts in the Qing dynasty (1644–1911) of China. *Clim. Past,* 16**,** 911-931.

Liu, W., Huang, B., Thorne, P. W., Banzon, V. F., Zhang, H.-M., Freeman, E., Lawrimore, J., Peterson, T. C., Smith, T. M. & Woodruff, S. D. 2015. Extended Reconstructed Sea Surface Temperature Version 4 (ERSST.v4): Part II. Parametric and Structural Uncertainty Estimations. *Journal of Climate,* 28**,** 931-951.

Liu, Y., Cobb, K. M., Song, H., Li, Q., Li, C.-Y., Nakatsuka, T., An, Z., Zhou, W., Cai, Q., Li, J., Leavitt, S. W., Sun, C., Mei, R., Shen, C.-C., Chan, M.-H., Sun, J., Yan, L., Lei, Y., Ma, Y., Li, X., Chen, D. & Linderholm, H. W. 2017. Recent enhancement of central Pacific El Niño variability relative to last eight centuries. *Nature Communications,* 8**,** 15386.

Accepted Article

Luan, Y., Braconnot, P., Yu, Y., Zheng, W. & Marti, O. 2012. Early and mid-Holocene climate in the tropical Pacific: seasonal cycle and interannual variability induced by insolation changes. *Clim. Past,* 8**,** 1093-1108.

Lucena, D. B., Servain, J. & Gomes Filho, M. F. 2011. Rainfall Response in Northeast Brazil from Ocean Climate Variability during the Second Half of the Twentieth Century. *Journal of Climate,* 24**,** 6174-6184.

McGregor, S., Timmermann, A., England, M. H., Elison Timm, O. & Wittenberg, A. T. 2013. Inferred changes in El Niño–Southern Oscillation variance over the past six centuries. *Clim. Past,* 9**,** 2269-2284.

McGregor, S., Timmermann, A. & Timm, O. 2010. A unified proxy for ENSO and PDO variability since 1650. *Clim. Past,* 6**,** 1-17.

McPhaden, M. J. 1999. Genesis and Evolution of the 1997-98 El Niño. *Science,* 283**,** 950-954.

McPhaden, M. J., Santoso, A. & Cai, W. 2020. *El Niño Southern Oscillation in a Changing Climate*, John Wiley & Sons.

McPhaden, M. J., Timmermann, A., Widlansky, M. J., Balmaseda, M. A. & Stockdale, T. N. 2015. The Curious Case of the EL Niño That Never Happened: A Perspective from 40 Years of Progress in Climate Research and Forecasting. *Bulletin of the American Meteorological Society,* 96**,** 1647-1665.

Meehl, G. A., Teng, H. & Branstator, G. 2006. Future changes of El Niño in two global coupled climate models. *Climate Dynamics,* 26**,** 549-566.

Morice, C. P., Kennedy, J. J., Rayner, N. A., Winn, J. P., Hogan, E., Killick, R. E., Dunn, R. J. H., Osborn, T. J., Jones, P. D. & Simpson, I. R. 2021. An Updated Assessment of Near-Surface Temperature Change From 1850: The HadCRUT5 Data Set. *Journal of Geophysical Research: Atmospheres,* 126**,** e2019JD032361.

Neelin, J. D., Battisti, D. S., Hirst, A. C., Jin, F.-F., Wakata, Y., Yamagata, T. & Zebiak, S. E. 1998. ENSO theory. *Journal of Geophysical Research: Oceans,* 103**,** 14261-14290.

O'Carroll, A. G., Armstrong, E. M., Beggs, H. M., Bouali, M., Casey, K. S., Corlett, G. K., Dash, P., Donlon, C. J., Gentemann, C. L. & Hoyer, J. L. 2019. Observational needs of sea surface temperature. *Frontiers in Marine Science,* 6.

Ohba, M. & Ueda, H. 2009. Role of Nonlinear Atmospheric Response to SST on the Asymmetric Transition Process of ENSO. *Journal of Climate,* 22**,** 177-192.

Ohba, M. & Watanabe, M. 2012. Role of the Indo-Pacific Interbasin Coupling in Predicting Asymmetric ENSO Transition and Duration. *Journal of Climate,* 25**,** 3321-3335.

Okumura, Y. M. & Deser, C. 2010. Asymmetry in the Duration of El Niño and La Niña. *Journal of Climate,* 23**,** 5826-5843.

Parker, W. S. 2016. Reanalyses and Observations: What's the Difference? *Bulletin of the American Meteorological Society,* 97**,** 1565-1572.

Parkinson, C. L. 2003. Aqua: an Earth-Observing Satellite mission to examine water and other climate variables. *IEEE Transactions on Geoscience and Remote Sensing,* 41**,** 173-183.

Philander, S. 1990. El Niño, La Niña, and the Southern Oscillation. S. George Philander. Academic Press, San Diego, CA, 1989. x, 293 pp., illus. $59.50. International geophysics series, vol. 46. *Science,* 248**,** 904-905.

Accepted Article

Phillips, J., Rajagopalan, B., Cane, M. & Rosenzweig, C. 1999. The role of ENSO in determining climate and maize yield variability in the U.S. cornbelt. *International Journal of Climatology,* 19**,** 877-888.

Pillar, H. R., Johnson, H. L., Marshall, D. P., Heimbach, P. & Takao, S. 2018. Impacts of Atmospheric Reanalysis Uncertainty on Atlantic Overturning Estimates at 25°N. *Journal of Climate,* 31**,** 8719-8744.

Poli, P., Hersbach, H., Dee, D. P., Berrisford, P., Simmons, A. J., Vitart, F., Laloyaux, P., Tan, D. G. H., Peubey, C., Thépaut, J.-N., Trémolet, Y., Hólm, E. V., Bonavita, M., Isaksen, L. & Fisher, M. 2016. ERA-20C: An Atmospheric Reanalysis of the Twentieth Century. *Journal of Climate,* 29**,** 4083-4097.

Predybaylo, E., Stenchikov, G. L., Wittenberg, A. T. & Zeng, F. 2017. Impacts of a Pinatubo-size volcanic eruption on ENSO. *Journal of Geophysical Research: Atmospheres,* 122**,** 925-947.

Qian, C., Wu, Z., Fu, C. & Wang, D. 2011. On changing El Niño: A view from time-varying annual cycle, interannual variability, and mean state. *Journal of Climate,* 24**,** 6486-6500.

Quinn, W. H. 1993. The Large-Scale ENSO Event, the El Nino and Other Important Regional Features. *Bull. Inst. fr. études an dines,* 22**,** 13-34.

Quinn, W. H., Neal, V. T. & Antunez De Mayolo, S. E. 1987. El Niño occurrences over the past four and a half centuries. *Journal of Geophysical Research: Oceans,* 92**,** 14449-14461.

Quinn, W. H., Zopf, D. O., Short, K. S. & Yang, R. K. 1978. Historical trends and statistics of the Southern Oscillation, El Niño, and Indonesian droughts. *Fish. Bull,* 76**,** 663-678.

Ramesh, N. & Murtugudde, R. 2013. All flavours of El Niño have similar early subsurface origins. *Nature Climate Change,* 3**,** 42-46.

Ray, S. & Giese, B. S. 2012. Historical changes in El Niño and La Niña characteristics in an ocean reanalysis. *Journal of Geophysical Research: Oceans,* 117.

Rayner, N. A., Brohan, P., Parker, D. E., Folland, C. K., Kennedy, J. J., Vanicek, M., Ansell, T. J. & Tett, S. F. B. 2006. Improved Analyses of Changes and Uncertainties in Sea Surface Temperature Measured In Situ since the Mid-Nineteenth Century: The HadSST2 Dataset. *Journal of Climate,* 19**,** 446-469.

Rayner, N. A., Parker, D. E., Horton, E. B., Folland, C. K., Alexander, L. V., Rowell, D. P., Kent, E. C. & Kaplan, A. 2003. Global analyses of sea surface temperature, sea ice, and night marine air temperature since the late nineteenth century. *Journal of Geophysical Research: Atmospheres,* 108.

Reynolds, R. W. 1988. A Real-Time Global Sea Surface Temperature Analysis. *Journal of Climate,* 1**,** 75-87.

Reynolds, R. W., Rayner, N. A., Smith, T. M., Stokes, D. C. & Wang, W. 2002. An Improved In Situ and Satellite SST Analysis for Climate. *Journal of Climate,* 15**,** 1609-1625.

Reynolds, R. W. & Smith, T. M. 1994. Improved Global Sea Surface Temperature Analyses Using Optimum Interpolation. *Journal of Climate,* 7**,** 929-948.

Rienecker, M. M., Suarez, M. J., Gelaro, R., Todling, R., Bacmeister, J., Liu, E., Bosilovich, M. G., Schubert, S. D., Takacs, L., Kim, G.-K., Bloom, S., Chen, J.,

Accepted Article

Collins, D., Conaty, A., da Silva, A., Gu, W., Joiner, J., Koster, R. D., Lucchesi, R., Molod, A., Owens, T., Pawson, S., Pegion, P., Redder, C. R., Reichle, R., Robertson, F. R., Ruddick, A. G., Sienkiewicz, M. & Woollen, J. 2011. MERRA: NASA's Modern-Era Retrospective Analysis for Research and Applications. *Journal of Climate,* 24**,** 3624-3648.

Ropelewski, C. F. & Jones, P. D. 1987. An Extension of the Tahiti–Darwin Southern Oscillation Index. *Monthly Weather Review,* 115**,** 2161-2165.

Saha, S., Moorthi, S., Pan, H.-L., Wu, X., Wang, J., Nadiga, S., Tripp, P., Kistler, R., Woollen, J., Behringer, D., Liu, H., Stokes, D., Grumbine, R., Gayno, G., Wang, J., Hou, Y.-T., Chuang, H.-y., Juang, H.-M. H., Sela, J., Iredell, M., Treadon, R., Kleist, D., Van Delst, P., Keyser, D., Derber, J., Ek, M., Meng, J., Wei, H., Yang, R., Lord, S., van den Dool, H., Kumar, A., Wang, W., Long, C., Chelliah, M., Xue, Y., Huang, B., Schemm, J.-K., Ebisuzaki, W., Lin, R., Xie, P., Chen, M., Zhou, S., Higgins, W., Zou, C.-Z., Liu, Q., Chen, Y., Han, Y., Cucurull, L., Reynolds, R. W., Rutledge, G. & Goldberg, M. 2010. The NCEP Climate Forecast System Reanalysis. *Bulletin of the American Meteorological Society,* 91**,** 1015-1058.

Sanchez, S. C., Westphal, N., Haug, G. H., Cheng, H., Edwards, R. L., Schneider, T., Cobb, K. M. & Charles, C. D. 2020. A Continuous Record of Central Tropical Pacific Climate Since the Midnineteenth Century Reconstructed From Fanning and Palmyra Island Corals: A Case Study in Coral Data Reanalysis. *Paleoceanography and Paleoclimatology,* 35**,** e2020PA003848.

Santoso, A., Mcphaden, M. J. & Cai, W. 2017. The Defining Characteristics of ENSO Extremes and the Strong 2015/2016 El Niño. *Reviews of Geophysics,* 55**,** 1079-1129.

Singh, D., Seager, R., Cook, B. I., Cane, M., Ting, M., Cook, E. & Davis, M. 2018. Climate and the Global Famine of 1876–78. *Journal of Climate,* 31**,** 9445-9467.

Slingo, J. M. & Annamalai, H. 2000. 1997: The El Niño of the Century and the Response of the Indian Summer Monsoon. *Monthly Weather Review,* 128**,** 1778-1797.

Slivinski, L. C., Compo, G. P., Whitaker, J. S., Sardeshmukh, P. D., Giese, B. S., McColl, C., Allan, R., Yin, X., Vose, R., Titchner, H., Kennedy, J., Spencer, L. J., Ashcroft, L., Brönnimann, S., Brunet, M., Camuffo, D., Cornes, R., Cram, T. A., Crouthamel, R., Domínguez-Castro, F., Freeman, J. E., Gergis, J., Hawkins, E., Jones, P. D., Jourdain, S., Kaplan, A., Kubota, H., Blancq, F. L., Lee, T.-C., Lorrey, A., Luterbacher, J., Maugeri, M., Mock, C. J., Moore, G. W. K., Przybylak, R., Pudmenzky, C., Reason, C., Slonosky, V. C., Smith, C. A., Tinz, B., Trewin, B., Valente, M. A., Wang, X. L., Wilkinson, C., Wood, K. & Wyszyński, P. 2019. Towards a more reliable historical reanalysis: Improvements for version 3 of the Twentieth Century Reanalysis system. *Quarterly Journal of the Royal Meteorological Society,* 145**,** 2876-2908.

Smith, C. A. & Sardeshmukh, P. D. 2000. The effect of ENSO on the intraseasonal variance of surface temperatures in winter. *International Journal of Climatology,* 20**,** 1543-1557.

Smith, T. M., Reynolds, R. W., Peterson, T. C. & Lawrimore, J. 2008. Improvements to NOAA's Historical Merged Land–Ocean Surface Temperature Analysis (1880–2006). *Journal of Climate,* 21**,** 2283-2296.

Accepted Article

Song, W., Dong, Q. & Xue, C. 2016. A classified El Niño index using AVHRR remote-sensing SST data. *International Journal of Remote Sensing,* 37**,** 403-417.

Stahle, D. W., D'Arrigo, R. D., Krusic, P. J., Cleaveland, M. K., Cook, E. R., Allan, R. J., Cole, J. E., Dunbar, R. B., Therrell, M. D. & Gay, D. A. 1998. Experimental dendroclimatic reconstruction of the Southern Oscillation. *Bulletin of the American Meteorological Society,* 79**,** 2137-2152.

Sullivan, A., Luo, J.-J., Hirst, A. C., Bi, D., Cai, W. & He, J. 2016. Robust contribution of decadal anomalies to the frequency of central-Pacific El Niño. *Scientific Reports,* 6**,** 38540.

Takahashi, K., Mosquera Vásquez, K. A. & Reupo Vélez, J. A. 2014. El Índice Costero El Niño (ICEN): historia y actualización.

Tardif, R., Hakim, G. J., Perkins, W. A., Horlick, K. A., Erb, M. P., Emile-Geay, J., Anderson, D. M., Steig, E. J. & Noone, D. 2019. Last Millennium Reanalysis with an expanded proxy database and seasonal proxy modeling. *Clim. Past,* 15**,** 1251-1273.

Thompson, D. W. J., Kennedy, J. J., Wallace, J. M. & Jones, P. D. 2008. A large discontinuity in the mid-twentieth century in observed global-mean surface temperature. *Nature,* 453**,** 646-649.

Thorne, P. W., Parker, D. E., Christy, J. R. & Mears, C. A. 2005. Uncertainties in Climate Trends: Lessons from Upper-Air Temperature Records. *Bulletin of the American Meteorological Society,* 86**,** 1437-1442.

Tian, Z., Li, T., Jiang, D. & Chen, L. 2017. Causes of ENSO weakening during the Mid-Holocene. *Journal of Climate,* 30**,** 7049-7070.

Tindall, J. C., Haywood, A. M. & Howell, F. W. 2016. Accounting for centennial-scale variability when detecting changes in ENSO: A study of the Pliocene. *Paleoceanography,* 31**,** 1330-1349.

Titchner, H. A. & Rayner, N. A. 2014. The Met Office Hadley Centre sea ice and sea surface temperature data set, version 2: 1. Sea ice concentrations. *Journal of Geophysical Research: Atmospheres,* 119**,** 2864-2889.

Trenberth, K. E. 1997. The Definition of El Niño. *Bulletin of the American Meteorological Society,* 78**,** 2771-2778.

Trenberth, K. E. & Hoar, T. J. 1997. El Niño and climate change. *Geophysical Research Letters,* 24**,** 3057-3060.

Trenberth, K. E. & Stepaniak, D. P. 2001. Indices of El Niño Evolution. *Journal of Climate,* 14**,** 1697-1701.

Troup, A. J. 1965. The 'southern oscillation'. *Quarterly Journal of the Royal Meteorological Society,* 91**,** 490-506.

Turkington, T., Timbal, B. & Rahmat, R. 2019. The impact of global warming on sea surface temperature based El Niño–Southern Oscillation monitoring indices. *International Journal of Climatology,* 39**,** 1092-1103.

Ummenhofer, C. C., Sen Gupta, A., Li, Y., Taschetto, A. S. & England, M. H. 2011. Multi-decadal modulation of the El Niño–Indian monsoon relationship by Indian Ocean variability. *Environmental Research Letters,* 6**,** 034006.

Accepted Article

van der Werf, G. R., Randerson, J. T., Collatz, G. J., Giglio, L., Kasibhatla, P. S., Avelino, A., Olsen, S. C. & Kasischke, E. S. 2004. Continental-scale partitioning of fire emissions during the 1997-2001 El Nino / La Nina period. *Science,* 303**,** 73-76.

van Oldenborgh, G. J., Hendon, H., Stockdale, T., L'Heureux, M., Coughlan de Perez, E., Singh, R. & van Aalst, M. 2021. Defining El Niño indices in a warming climate. *Environmental Research Letters,* 16**,** 044003.

Voskresenskaya, E. N. & Marchukova, O. V. 2017. Spatial classification of La Niña events. *Izvestiya, Atmospheric and Oceanic Physics,* 53**,** 111-119.

Wallace, J. M. & Gutzler, D. S. 1981. Teleconnections in the Geopotential Height Field during the Northern Hemisphere Winter. *Monthly Weather Review,* 109**,** 784-812.

Wang, B., Luo, X., Yang, Y.-M., Sun, W., Cane, M. A., Cai, W., Yeh, S.-W. & Liu, J. 2019. Historical change of El Niño properties sheds light on future changes of extreme El Niño. *Proceedings of the National Academy of Sciences,* 116**,** 22512-22517.

Wang, B., Wu, R. & Fu, X. 2000. Pacific–East Asian teleconnection: how does ENSO affect East Asian climate? *Journal of Climate,* 13**,** 1517-1536.

Wang, Z., Han, L., Ding, R. & Li, J. 2021. Evaluation of the performance of CMIP5 and CMIP6 models in simulating the South Pacific Quadrupole–ENSO relationship. *Atmospheric and Oceanic Science Letters,* 14**,** 100057.

Wilson, R., Cook, E., D'Arrigo, R., Riedwyl, N., Evans, M. N., Tudhope, A. & Allan, R. 2010. Reconstructing ENSO: the influence of method, proxy data, climate forcing and teleconnections. *Journal of Quaternary Science,* 25**,** 62-78.

Wittenberg, A. T. 2009. Are historical records sufficient to constrain ENSO simulations? *Geophysical Research Letters,* 36.

Wolde-Georgis, T. 1997. El Nino and drought early warning in Ethiopia. *Internet Journal of African Studies*.

Wolter, K. & Timlin, M. S. 2011. El Niño/Southern Oscillation behaviour since 1871 as diagnosed in an extended multivariate ENSO index (MEI.ext). *International Journal of Climatology,* 31**,** 1074-1087.

Woodruff, S. D., Slutz, R. J., Jenne, R. L. & Steurer, P. M. 1987. A Comprehensive Ocean-Atmosphere Data Set. *Bulletin of the American Meteorological Society,* 68**,** 1239-1250.

Woodruff, S. D., Worley, S. J., Lubker, S. J., Ji, Z., Eric Freeman, J., Berry, D. I., Brohan, P., Kent, E. C., Reynolds, R. W., Smith, S. R. & Wilkinson, C. 2011. ICOADS Release 2.5: extensions and enhancements to the surface marine meteorological archive. *International Journal of Climatology,* 31**,** 951-967.

Xie, S.-P., Hu, K., Hafner, J., Tokinaga, H., Du, Y., Huang, G. & Sampe, T. 2009. Indian Ocean Capacitor Effect on Indo–Western Pacific Climate during the Summer following El Niño. *Journal of Climate,* 22**,** 730-747.

Yeh, S.-W., Ham, Y.-G. & Lee, J.-Y. 2012. Changes in the Tropical Pacific SST Trend from CMIP3 to CMIP5 and Its Implication of ENSO. *Journal of Climate,* 25**,** 7764-7771.

Yeh, S.-W., Kug, J.-S., Dewitte, B., Kwon, M.-H., Kirtman, B. P. & Jin, F.-F. 2009. El Niño in a changing climate. *Nature,* 461**,** 511-514.

Accepted Article

Yu, J.-Y., Kao, H.-Y., Lee, T. & Kim, S. T. 2011. Subsurface ocean temperature indices for Central-Pacific and Eastern-Pacific types of El Niño and La Niña events. *Theoretical and Applied Climatology,* 103**,** 337-344.

Yu, L., Jin, X. & Weller, R. A. 2008. Multidecade Global Flux Datasets from the Objectively Analyzed Air-sea Fluxes (OAFlux) Project: Latent and sensible heat fluxes, ocean evaporation, and related surface meteorological variables. *OAFlux Project Tech. Rep. OA-2008-01,* 74.

Zanchettin, D., Franks, S. W., Traverso, P. & Tomasino, M. 2008. On ENSO impacts on European wintertime rainfalls and their modulation by the NAO and the Pacific multi-decadal variability described through the PDO index. *International Journal of Climatology,* 28**,** 995-1006.

Zhang, W., Wang, Y., Jin, F.-F., Stuecker, M. F. & Turner, A. G. 2015. Impact of different El Niño types on the El Niño/IOD relationship. *Geophysical Research Letters,* 42**,** 8570-8576.

Zhu, J., Huang, B., Marx, L., Kinter III, J. L., Balmaseda, M. A., Zhang, R.-H. & Hu, Z.-Z. 2012. Ensemble ENSO hindcasts initialized from multiple ocean analyses. *Geophysical Research Letters,* 39.

Zhu, J., Zhang, M., Zhang, Y., Zeng, X. & Xiao, X. 2018. Response of Tropical Terrestrial Gross Primary Production to the Super El Niño Event in 2015. *Journal of Geophysical Research: Biogeosciences,* 123**,** 3193-3203.

Zuo, H., Balmaseda, M. A., Tietsche, S., Mogensen, K. & Mayer, M. 2019. The ECMWF operational ensemble reanalysis–analysis system for ocean and sea ice: a description of the system and assessment. *Ocean Sci.,* 15**,** 779-808.

Accepted Article

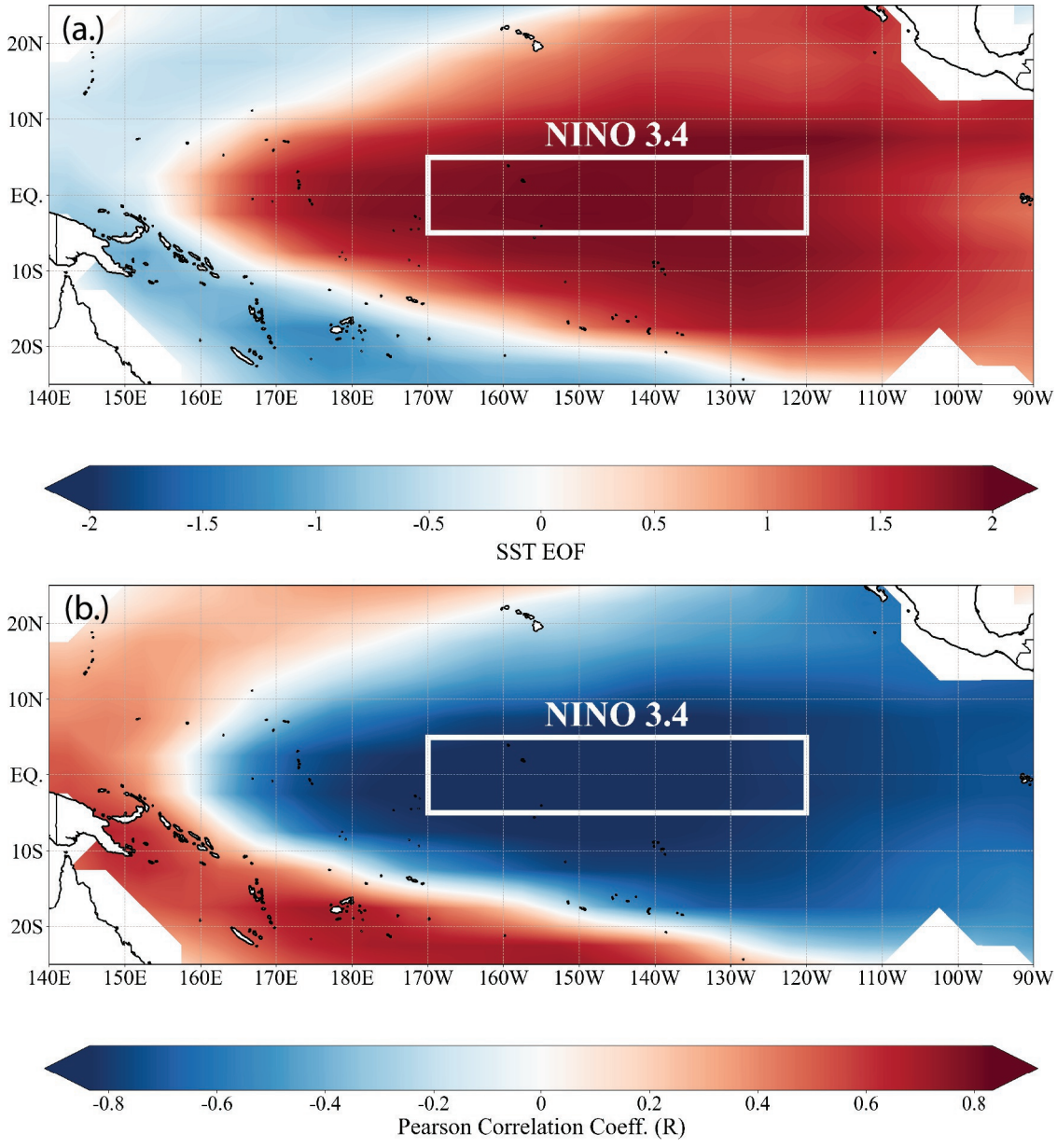

joc_7535_fig01-cmyk.eps

Accepted Article

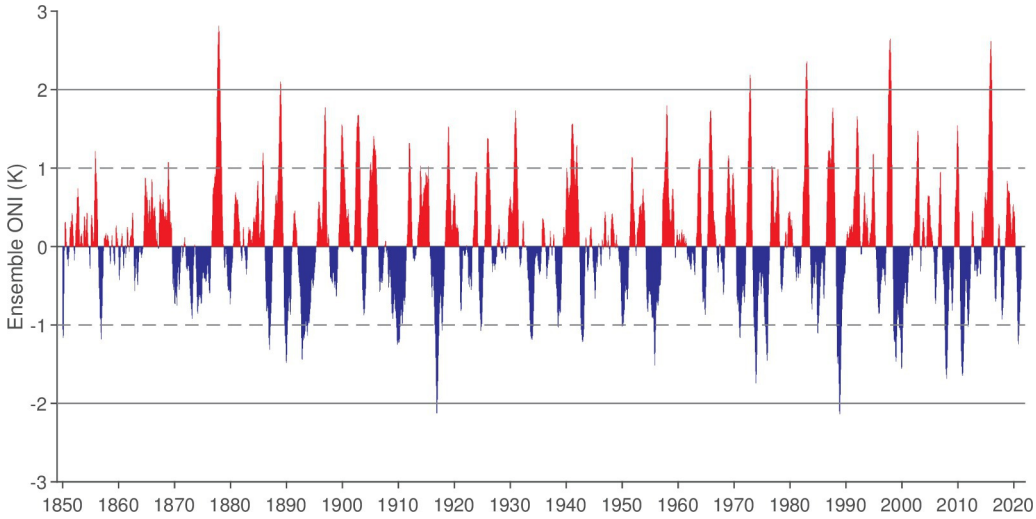

joc_7535_fig02-cmyk.eps

Accepted Article

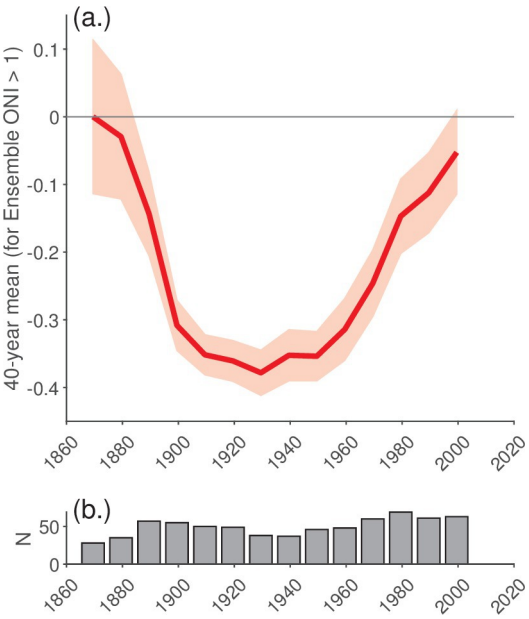

joc_7535_fig03-cmyk.eps

Accepted Article

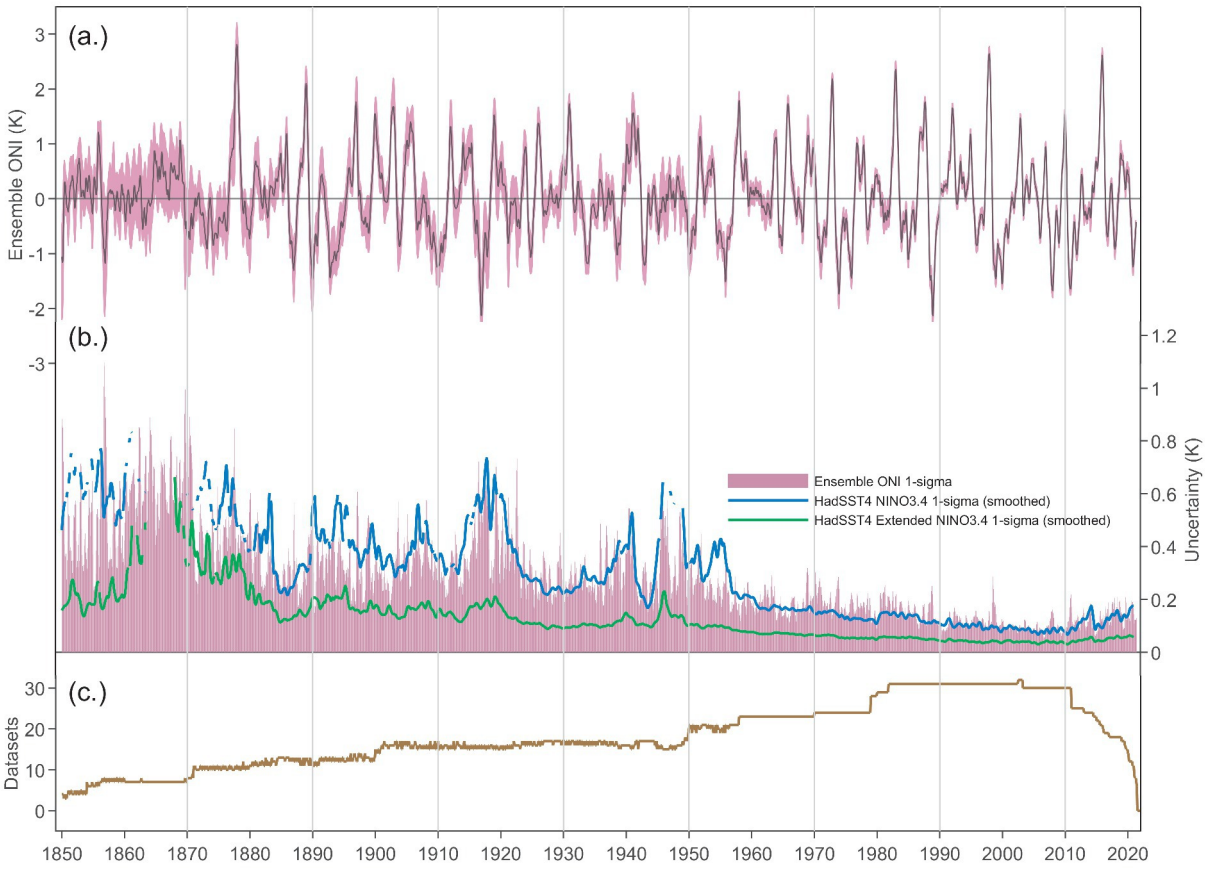

joc_7535_fig04-cmyk.eps

Accepted Article

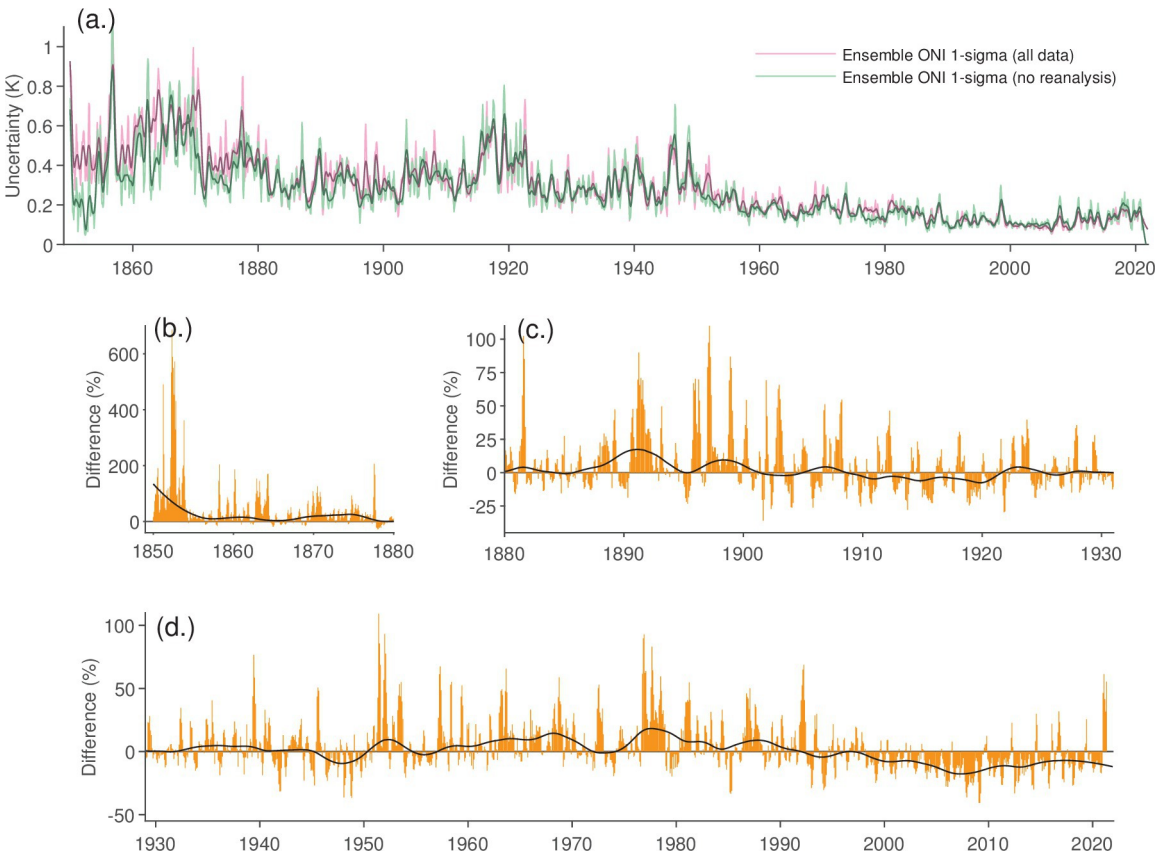

joc_7535_fig05-cmyk.eps

Accepted Article

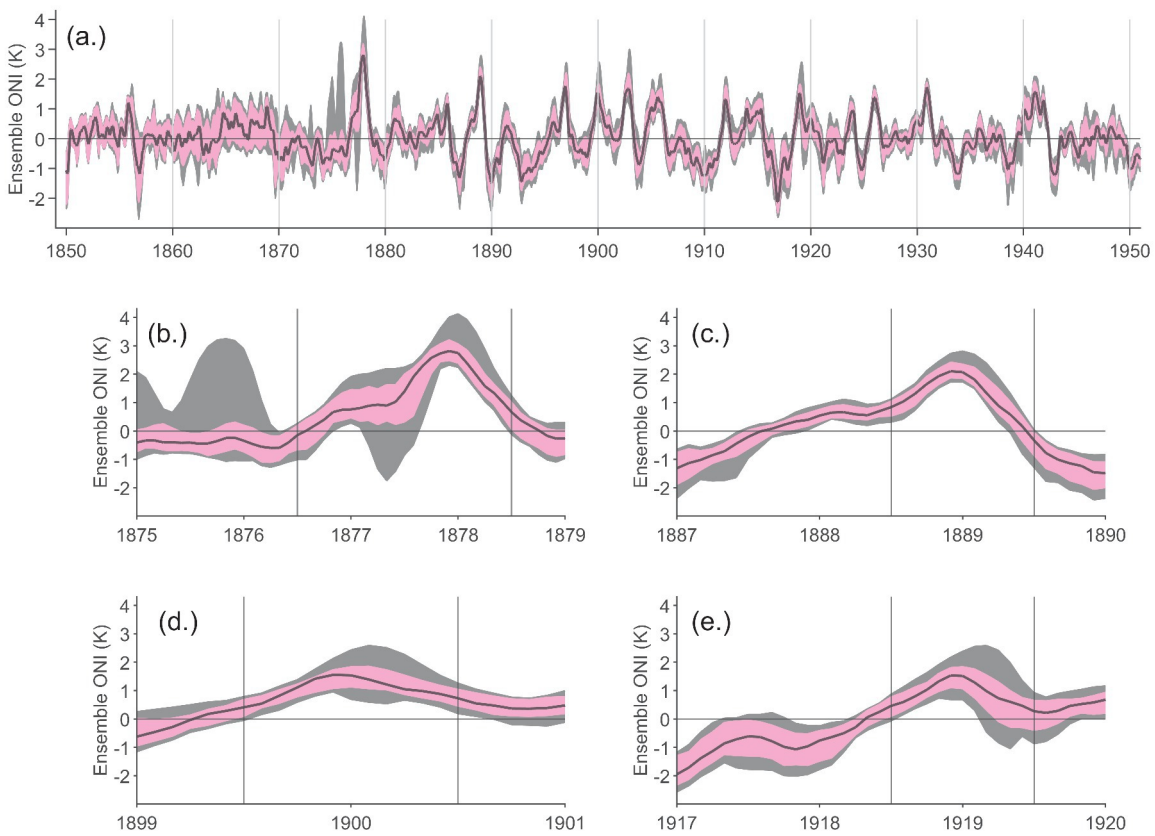

joc_7535_fig06-cmyk.eps

Accepted Article

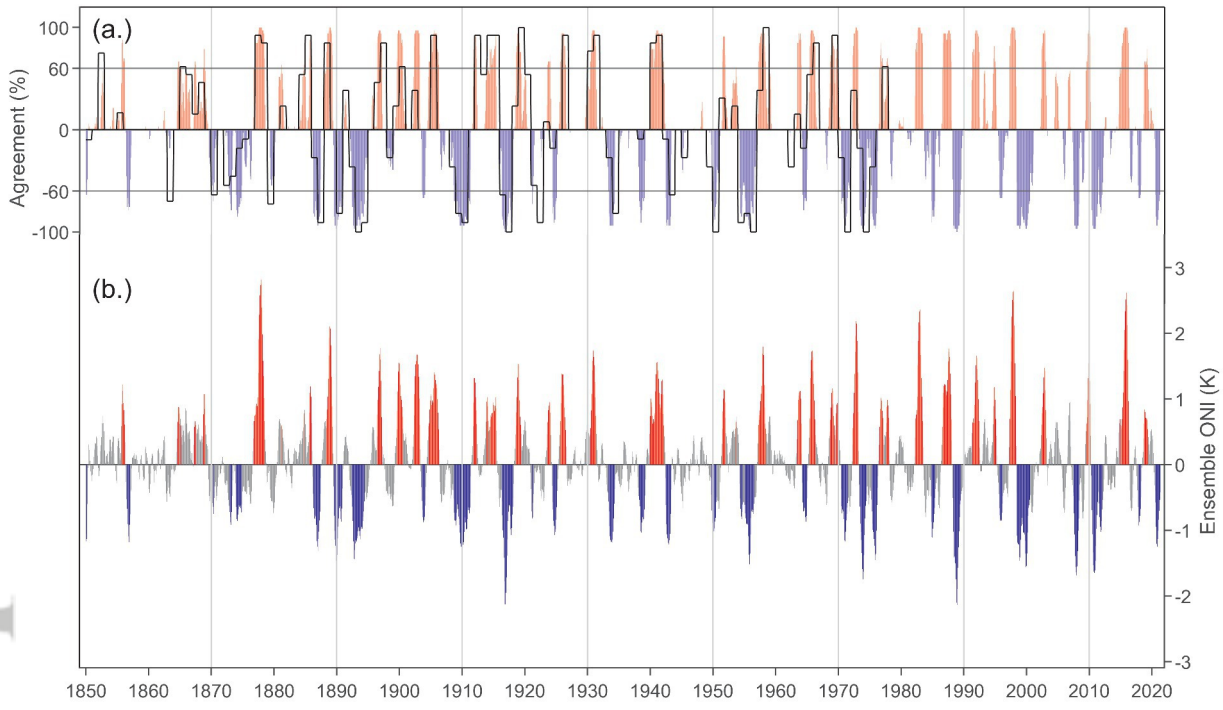

joc_7535_fig07-cmyk.eps

Accepted Article

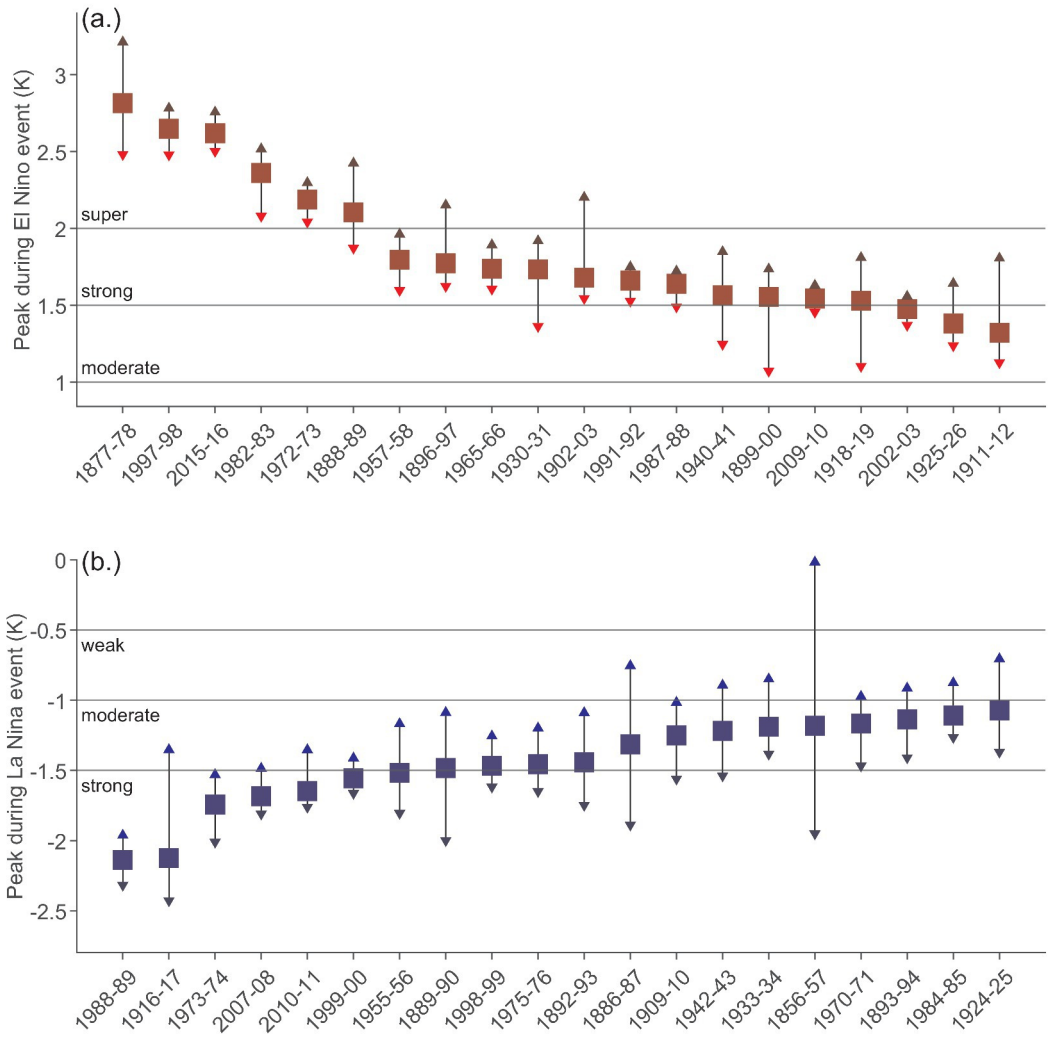

joc_7535_fig08-cmyk.eps

Accepted Article

Title: The Ensemble Oceanic Nino Index

Authors: Eric J. Webb, Brian I. Magi*

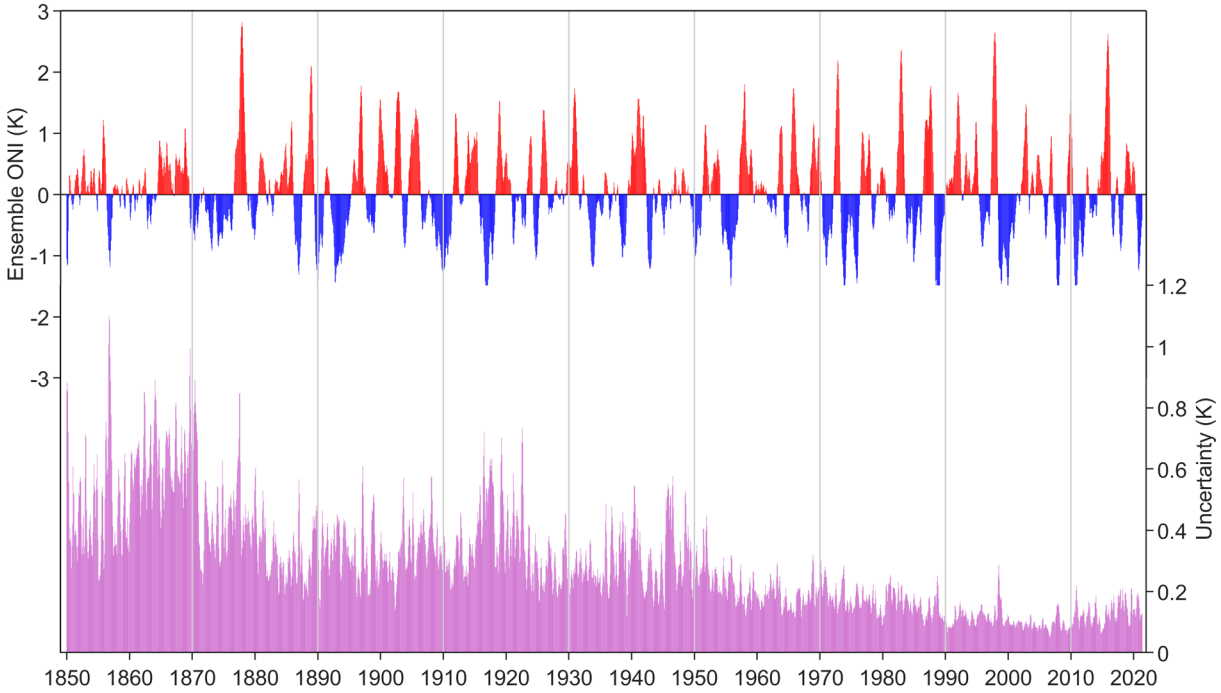

Caption: El Nino Southern Oscillation (ENSO) is a well-known mode of climate variability that affects weather around the world. A way to document ENSO state is with the sea surface temperature (SST) anomaly in the tropical Pacific Ocean. SST has been measured since at least the mid-1800s, and we leverage an ensemble of available datasets to produce an ENSO index with accompanying uncertainty from 1850 to present. We call our ENSO index the Ensemble Oceanic Nino Index or Ensemble ONI.

Accepted Article

Table 1. The 32 input datasets used to calculate the Ensemble ONI. The 15 datasets listed with an asterisk are reanalysis or include an element of model/interpolation to supplement observations.

Dataset	Range	Resolution	Reference
HADISST2.1	1850-2010	1x1°	Titchner and Rayner (2014)
NOAA 20CRv3*	1850-2015	1x1°	Slivinski *et al.* (2019)
COBE SST2	1850-2018	1x1°	Hirahara *et al.* (2014)
HADSST4	1850-2020	5x5°	Kennedy *et al.* (2019)
NOAA 20CRv2c*	1851-2014	2x2°	Compo *et al.* (2011)
ERSSTv5	1854-2020	2x2°	Huang *et al.* (2017)
ERSSTv4	1854-2020	2x2°	Huang *et al.* (2015)
Kaplan Extended v2	1856-2020	5x5°	Kaplan *et al.* (1998)
HADISST	1870-2020	1x1°	Rayner *et al.* (2003)
NOAA 20CRv2*	1871-2012	2x2°	Compo *et al.* (2011)
SODAv2.2.4	1871-2010	0.5x0.5°	Giese and Ray (2011)
ICOADSv3	1878-2019	2x2°	Freeman *et al.* (2017)
COBE SST	1891-2020	1x1°	Ishii *et al.* (2005)
ERA-20C*	1900-2010	1x1°	Poli *et al.* (2016)
ERA-20CM*	1900-2010	1x1°	Hersbach *et al.* (2015)
CERA-20C*	1901-2010	1x1°	Laloyaux *et al.* (2018)
NCEP-R1*	1948-2020	2.5x2.5°	Kalnay *et al.* (1996)
HADSST2	1950-2012	5x5°	Rayner *et al.* (2006)
HADSST3	1950-2020	5x5°	Kennedy *et al.* (2011a)
ERSSTv3b	1880-2020	2x2°	Smith *et al.* (2008)
ORAS5*	1958-2018	0.25x0.25°	Zuo *et al.* (2019)
WHOI OA Flux v3*	1958-2019	2.5x2.5°	Yu *et al.* (2008)
CAC SST	1970-2003	2x2°	Reynolds (1988)
ERA-5*	1979-2019	0.28x0.28°	Hersbach *et al.* (2020)
NCEP CFSR*	1979-2015	0.5x0.5°	Saha *et al.* (2010)
NCEP DOE R2*	1979-2020	2x2°	Kanamitsu *et al.* (2002)
ERA-Interim*	1979-2019	1x1°	Dee *et al.* (2011)
NASA MERRA*	1979-2016	0.5x0.66°	Rienecker *et al.* (2011)
NASA MERRAv2*	1980-2016	0.5x0.625°	Gelaro *et al.* (2017)
OISSTv1	1981-2003	1x1°	Reynolds and Smith (1994)
OISSTv2.1	1981-2020	1x1°	Reynolds *et al.* (2002)
AQUA-MODIS	2002-2020	1x1°	Parkinson (2003)

Accepted Article

Table 2. 33 literature-based definitions of ENSO events

	Institution/Reference	Criteria Amplitude	Criteria Length
1	Ashok *et al.* (2007)	> +/- 0.7σ SST	3 tri-monthlies
2	Australian Bureau of Meteorology	> +/- 0.8°C SST	Any month
3	Bove *et al.* (1998)	> +/- 0.5°C SST	6 consecutive pentads
4	Chen *et al.* (2004), Yu *et al.* (2011)	> +/- 1.0°C SST	Any month
5	Coelho *et al.* (2002)	> +/- 2.0°C SST	Any month
6	Gergis and Fowler (2005)	> +/- 0.5°C SST	6 consecutive months
7	Hanley *et al.* (2003)	El Nino: 25th %ile, La Nina: 75th %ile	Any month
8	Hanley *et al.* (2003)	> +/- 1.0σ SST	4 consecutive months
9	Luan *et al.* (2012)	> +/- 1.2σ SST	Any month
10	Lucena *et al.* (2011)	> +/- 0.5°C SST	2 consecutive tri-monthlies
11	McGregor *et al.* (2010)	> +/- 0.5σ SST	Any month
12	Meehl *et al.* (2006), Tian *et al.* (2017)	> +/- 1.0σ SST	1 tri-monthly

Accepted Article

13	NOAA Climate Prediction Center	> +/- 0.5°C SST	5 consecutive tri-monthlies
14	Predybaylo *et al.* (2017)	> +/- 1.4°C SST	1 tri-monthly
15	Predybaylo *et al.* (2017)	> +/- 1.0°C SST	1 tri-monthly
16	Santoso *et al.* (2017)	> +/- 0.5σ SST	1 tri-monthly
17	Zanchettin *et al.* (2008), Sullivan *et al.* (2016)	> +/- 0.5°C SST	1 pentad
18	Takahashi *et al.* (2014)	> +/- 0.4°C SST	3 consecutive months
19	Takahashi *et al.* (2014)	> +/- 1.0°C SST	3 consecutive months
20	Trenberth and Hoar (1997)	> +/- 0.4°C SST	6 consecutive tri-monthlies
21	Wang *et al.* (2000)	> +/- 0.5°C SST	8 months
22	Wang *et al.* (2019)	> +/- 0.6°C SST	1 pentad
23	Wolter and Timlin (2011)	El Nino: 30th %ile, La Nina: 70th %ile	1 bi-monthly
24	Yeh *et al.* (2009)	> +/- 0.5°C SST	1 tri-monthly
25	Zanchettin *et al.* (2008)	> +/- 0.4°C SST	1 pentad
26	Zhang *et al.* (2015)	> +/- 0.6σ SST	1 tri-monthly
27	Phillips *et al.* (1999)	> +/- 0.7σ SST	4-month period
28	Song *et al.* (2016)	> +/- 0.5σ SST	4 consecutive months

29	Qian *et al.* (2011), Voskresenskaya and Marchukova (2017)	> +/- 0.5°C SST	5 consecutive months
30	Hendon *et al.* (2009)	> +/- 0.7σ SST	1 tri-monthly
31	Kao and Yu (2009)	> +/- 1.0σ SST	3 consecutive months
32	JMA	> +/- 0.5σ SST	6 consecutive pentads
33	Turkington *et al.* (2019)	> +/- 0.25°C SST	5 successive tri-monthlies

Accepted Article